Nuclear Roles of Spliceosome-Associated microRNAs in Neuronal Cancer Cells

Shelly Mahlab Aviv , Keren Or Swissa , Maram Arafat , Keren Zohar , Ayelet R Peretz , Michal Linial * , Ruth Sperling *

Posted Date: 8 August 2025

doi: 10.20944/preprints202508.0564.v1

Keywords: lncRNA; Antisense; nuclear miRNA; spliceosomal-miRNA; splicing; pre-miRNA; miRNA biogenesis; miRCancer

 doi:10.20944/preprints202508.0564.v1

Article

Nuclear Roles of Spliceosome-Associated microRNAs in Neuronal Cancer Cells

Shelly Mahlab-Aviv [1], Keren Or Swissa [2], Maram Arafat [2], Keren Zohar [1], Ayelet, R. Peretz [2], Michal Linial [1,*] and Ruth Sperling [2,*]

[1] Department of Biological Chemistry, The Hebrew University of Jerusalem, 91904 Israel

[2] Department of Genetics, The Life Science Institute, The Hebrew University of Jerusalem, 91904 Israel

* Correspondence: michall@mail.huji.ac.il (M.L.); r.sperling@mail.huji.ac.il (R.P.);
Tel.: +972-54-8820035 (M.L.); +972-54-882-0311 (R.P.); Fax: +972-2-6523429 (M.L.); +972-2-658-6975 (R.P.)

Abstract

MicroRNAs (miRNAs) are well-known for regulating translation in the cytoplasm, yet their roles in the nucleus remain poorly understood. Previously, we identified spliceosome-associated miRNAs implicated in tumorigenesis and metastasis in breast cancer models. Here, we investigate their nuclear functions in immortalized human cortical neurons (HCN) cell line, along with brain cancer derived cell lines of glioblastoma (U87MG) and neuroblastoma (SH-SY5Y) that are widely used as models for brain cancer research. Our findings reveal that spliceosome-associated miRNAs mark neuronal cancer cells and uncover novel nuclear targets. Interestingly, some spliceosomal miRNAs exhibit opposing regulatory effects in the nucleus compared to the cytoplasm, while some portray potential novel nuclear functions. A notable example is miR-99b, which overlaps the 5′ splice junction of the poorly characterized long non-coding RNA (lncRNA) **SPACA6-AS1** and, through base-pairing, enhances SPACA6-AS1 pre-mRNA levels. These findings highlight the diverse and context-dependent functions of nuclear miRNAs in gene regulation and cancer progression, expanding our understanding of their regulatory potential beyond the cytoplasm.

Keywords: lncRNA; Antisense; nuclear miRNA; spliceosomal-miRNA; splicing; pre-miRNA; miRNA biogenesis; miRCancer

Introduction

MicroRNA (miRNAs) are small, ~22 nt long, non-coding RNA (ncRNA) molecules involved in regulating gene expression, and changes in miRNA expression have been associated with numerous human diseases including cancer [1,2]. The canonical role of miRNAs in mammals is in inhibiting translation, through base-pairing of miRNAs to the 3′-UTR of the target mRNA transcripts in the cytoplasm [3–7]. In humans, many miRNA genes are located in gene introns and their canonical biogenesis from Pol II transcripts involves the nuclear cleavage of the pri-miRNA by Drosha, complexed with DGCR8 to generate the precursor (pre) miRNA stem-loop molecule of 70-80 bases [8–12]. Along with the biogenesis of miRNAs, the pre-miRNA is exported to the cytoplasm, where it is cleaved by Dicer yielding a mature miRNA, which is loaded on the RNA Induced Silencing Complex (RISC) [3,4,13]. The RISC-bound miRNAs act in targeting mRNAs in the cytoplasm [7]. Changes in the level of miRNAs expression has the potential to perturb cellular pathways leading to human diseases such as neurodegenerative diseases, chronic inflammation, metabolic disorders, and cancer onset and progression [1,2,14,15].

The role of miRNAs in the progression of cancer has been established. Most studies focus on the major cancer related miRNAs that are known to affect main cancer hallmarks including proliferation, apoptosis, invasion, differentiation and more [16]. The most direct effect of miRNAs in cancer and specifically in brain-related cancers such as gliomas and medulloblastomas concerns the targeting of oncogenes or tumor suppressor genes. For instance, miR-21 is frequently upregulated in glioblastoma

 doi:10.20944/preprints202508.0564.v1

multiforme (GBM) and targets PTEN and PDCD4 resulting in cell proliferation and tumor progression [17]. Importantly, miRNAs are not only involved in early phases but can impact cell invasive and metastatic properties. For example, miR-10b has been shown to enhance invasive capabilities of glioma cells by targeting HOXD10 [18]. While most abundant miRNAs are often overexpressed in cancer as a result of relaxation in epigenetic marks, other miRNAs are suppressed. For example, the downregulation of miR-9 has been associated with increased metastatic potential in medulloblastomas, by allowing the full capacity of the metastasis-associated gene E-cadherin. On the other hand, miR-34a is often downregulated in GBM and inhibits tumor growth by targeting genes involved in cell cycle regulation and apoptosis (e.g., Notch1 and Bcl-2). Thus, restoring the expression of miR-34a (miRNA mimics) has shown promise in reducing tumor growth in preclinical models of GBM. miR-34a inhibits glioblastoma growth by targeting multiple oncogenes [19].

The impact of miRNAs to suppress or induce tumorigenesis rely on multiple features related to the expression level and miRNA maturation. The measured level of miRNAs and their composition are a consequence of miRNA biogenesis, subcellular location (e.g., partition of the cellular amounts between the nuclei and cytosol [20]. A crosstalk of RNA binding proteins and miRNAs provides another regulatory axis in cancer related post-transcriptional control [21].

The finding of mature miRNAs in the nucleus [22–26], suggested nuclear functions for miRNA in addition to the classical cytoplasmic ones [27,28], and active process of shuttling of miRNAs from the cytoplasm to the nucleus were demonstrated [29,30]. Although the functions of miRNAs in the nucleus are not yet fully understood [26], the involvement of miRNA in a number of processes was documented. This includes regulation of ncRNAs [31–35], transcriptional silencing [36,37], activation [38–41], and inhibition [37]. Furthermore, analysis of miRNA-mRNA-AGO interactions, revealed substantial AGO-miRNA mapping to intronic sequences [42]. A large fraction of miRNA genes is located in introns of coding genes, while many are expressed from their own PolII promoters [6,43,44]. For most intronic miRNAs, the mRNA and such miRNA can be expressed from the same primary transcript. However, when the pri-miRNA is located in an exon or overlaps a splice site, at any specific time only the mRNA or the miRNA can be generated from the single transcript. In the case of alternative splicing (AS), the expression of both the mRNA and the miRNA from the same transcript is possible [44]. Furthermore, several studies showed links between splicing and miRNA processing [30,45–49].

Splicing and AS play a major role in the regulation of gene expression in mammals, and changes in AS occur in many human diseases including cancer [50–53]. Splicing occurs in the cell nucleus within a huge (21 MDa) and highly dynamic molecular machine known as the endogenous spliceosome – the supraspliceosome, which is involved in all nuclear processing activities of pre-mRNAs [54,55]. It is composed of four native spliceosomes, which are connected by the pre-mRNA [56,57]. The entire repertoire of nuclear pre-mRNAs, independent of their length and number of introns, is individually assembled in supraspliceosomes, which offers coordination and regulation of pre-mRNA processing events [54,55]. Furthermore, miRNAs were found within the endogenous spliceosome [58–60], where a cross-talk between pre-mRNA splicing and miRNA processing was demonstrated [49,58–61].

Here, we analysed miRNA sequences found in supraspliceosomes (SF) isolated from neuronal cancer cells by RNA-Seq. The analyses revealed a large collection of spliceosomal miRNA sequences found in each of the tested neuronal cancer cells, where the amount and type of SF-miRNA signify each of the neuronal cancer cell lines. Furthermore, novel roles for SF-miRNAs which is different from their classical cytoplasmic roles were identified. A notable example involves spliceosomal miR-99b, which overlaps the 5′ splice junction of the poorly-characterized lncRNA SPACA6-AS1. We have shown that SF-miR-99b, which base-pairs with the 5′ splice site of SPSCS6-AS1 enhances the level of SPACA6-AS1 pre-mRNA. These findings highlight the implications of miRNA position on transcriptional regulation and point to novel cancer-related nuclear targets.

Materials and Methods

 doi:10.20944/preprints202508.0564.v1

Cell lines

Spliceosomes and RNA were isolated from the following cell-lines: HCN-2 human cortical neuron cell line (female originated, doubling time 48 hrs), , used as a model for healthy cell function (ATCC, CRL-3592); U87MG, a human glioblastoma cell line (ATCC, HTB-14), is one of the most commonly used glioblastoma cell lines (male origin), with doubling time of approximating 34 hrs; and SH-SY5Y, a human neuroblastoma cell line derived from a bone marrow biopsy (ATCC, CRL-2266; female originated with 27 hrs doubling time), commonly used in cancer research. It exhibits neuronal properties and can be differentiated into more mature neuron-like cells. Cell lines were cultured according to the ATCC protocols for cell maintenance.

Isolation of Supraspliceosomes

Supraspliceosomes were prepared, as previously described [56], from nuclear supernatants enriched in supraspliceosomes from the following cell-lines: HCN, U87MG and SH-SY5Y. Briefly, nuclear supernatants were prepared from purified cell nuclei by microsonication of the nuclei and precipitation of the chromatin in the presence of excess of tRNAs. All isolation steps were conducted at 4°C. The nuclear supernatant was fractionated on 10-45% (vol/vol) glycerol gradients. Centrifugations were carried out at 4°C in an SW41 rotor run at 41 krpm for 90 min [or an equivalent $\omega^2 t = 2500$ (ω is in krpm; t is in hr)]. The gradients were calibrated using the tobacco mosaic virus as a 200S sedimentation marker. Supraspliceosome peak fractions were confirmed by Western Blot (WB) and by electron microscopy visualization.

Protein Detection

Western blotting (WB) analyses were performed as previously described [62]. We used anti-alpha tubulin antibodies AB-7291 (abcam) visualized with horseradish peroxidase conjugated to affinity-pure Goat anti-Mouse IgG (H+L; Jackson Immunoreaserch, 1:5000), and anti-H3 histone antibodies (63) visualized with horseradish peroxidase conjugated to affinity-pure Goat anti-Mouse IgG (H+L; Jackson Immunoreaserch, 1:5000) used as previously described [63], and (09-838, Merck), visualized with horseradish peroxidase conjugated to affinity-pure Goat anti-rabbit IgG (H+L; Jackson Immunoreaserch, 1:5000).

RNA Isolation from Supraspliceosomes and Deep Sequencing

RNA was extracted as previously described [56] from supraspliceosomes prepared from each of the different three neuronal cell-lines: the two neuronal cancer cells at different stages of malignancy: U87MG and SH-SY5Y; and the non-tumorigenic neuronal cell-line HCN. The integrity of the RNA was evaluated by an Agilent 2100 bioAnalyzer. For small RNA library construction, ~1 μg of RNA was used. After phosphatase and T4 polynucleotide kinase (PNK) treatments, the RNA was ethanol precipitated to enrich for small RNA, and small RNA libraries (in triplicates) were prepared according to NEBNext Small RNA Library Prep Set for Illumina (Multiplex Compatible) Library Preparation Manual. Adaptors were then ligated to the 5′ and 3′ ends of the RNA, and cDNA was prepared from the ligated RNA and amplified to prepare the sequencing library. The amplified sequences were purified on E-Gel® EX 4% Agarose gels (ThermoFisher #G401004), and sequences representing RNA smaller than 200 nt were extracted from the gel. The library was sequenced using the Illumina NextSeq 500 Analyzer. The sequencing data, after removal the adaptors and filtering out low quality sequences, were aligned to miRBase (Release 21). In addition, the filtered high-quality fragments were mapped to the human transcriptome of hg19 GTF file from UCSC provided by Galaxy. The hg19 transcriptome contains 963,559 exons from 45,314 transcripts. Sequences aligned to the miRNA genes as compiled in miRBAse are reported.

Next Generation Sequencing (NGS) Analysis

 doi:10.20944/preprints202508.0564.v1

RNA was extracted from three independent biological preparations from the supraspliceosome fractions from each of the different neuronal cell-lines. NGS was performed for each sample on small RNA (<200 nt) molecules using standard Illumina Protocol. Each library consisted of an average of 32, 34, and 47 million reads for HCN, U87MG and SH-SY5Y, respectively.

Raw data of the sequenced small RNA were trimmed using Cutadapt ver. 1.13. Low-quality reads were filtered out using FASTX toolkit. Reads from the SF were aligned against human genome hg19 and miRbase database (version 21) using TopHat 2.1.1, allowing 90% sequence identity and a maximum of two mismatches. Reads whose start or end position were mapped to miRNA genes were considered. High quality reads from the three SF preparations of each cell-line were combined. Out of the mapped reads, only reads of length ≥17 nt were considered. miRNA gene aligned sequences refer to all mapped, high-quality reads that are aligned to any of the pre-miRNA as defined by miRBase. For the rest of the analyses, only miRNA aligned sequence with ≥30 reads per all three cell-lines were considered. This threshold was used to ensure reliable support in view of the limited total reads assigned from supraspliceosomes. The analysed data were added to ArrayExpress and the data accession number is E-MTAB-15383. We have removed from total counts and normalization protocols the hsa-miR-6087 that was withdrawn from miRbase catalog.

Validation of Gene Expression

RT-PCR

RT-PCR was performed on RNA extracted from the cell-lines described above, and from nuclear supernatants of the above cells as described [64]. The following sets of primers for SPACA 6 NM_001316994.2 were used: Forward: 5′-GGGGAGAGGATGGAGAGCG-3′ and Reverse 5′-TCATTTTCTCCGCAGCATC-3′, with Tm 62°C for 35 cycles. The primers for pre-SPACA6-AS1 were: Forward, 5′-GGGCTCAAAGGTGAATCAGA-3′ and Reverse, 5′AGGGCCTTAGTGGAGGTCAT-3′, and run at Tm 58°C for 35 cycles. The identity of all PCR products was confirmed by sequencing. Each experiment was repeated at least 3 times. The relative abundance was quantified in view of the intensity of the ß-actin that was used as a control. The ß-actin Forward and Reverse primers, for an amplicon of 120 nt, are: 5′-CTGGAACGGTGAAGGTGACA-3′ and 5′-AAGGGACTTCCTGTAACAATGCA-3′, respectively.

Transfection and RNA Isolation

U87MG and SH-SY5Y cells were each grown in six-well plates. For downregulation of hsa-miR-99b, the cells were transfected with anti-hsa-miR-99b inhibitor AM11021 (ThermoFisher) according to manufacturer's instructions at 100 nM for 24 hrs. As controls we used the same cells transfected with anti-miR inhibitor, negative control #1 (AB-AM17000, ThermoFisher), and non-treated cells. For overexpression of miR-99b we used pre-miR has-miR-99b, PM11021 (AB-AM17100, ThermoFisher), and as negative control pre-miR negative control (AB-AM17110). Transfections were performed using Lipofectamine-2000 reagent (ThermoFisher).

For U87MG cells, nuclear RNA isolation was performed as previously described [49]. Briefly, 24 hrs post transfection, the six-well plates were washed with PBS followed by the addition of 175 μl of cold RLN buffer (50 mM Tris pH 8, 140 mM NaCl, 1.5 mM $MgCl_2$ and 0.5% NP40). The cells were then scraped and moved to an Eppendorf tube on ice for 5 min. Centrifugation for 2 min at 750 g, at 4°C, was then performed. The supernatant (cytoplasm) was transferred to a new tube and the pellet (nuclei) was centrifuged again. For SH-SY5Y cells, a modification of the above protocol was applied. Briefly, SH-SY5Y cells were seeded in 6-well plates. Washed with PBSx1 followed by addition of 175 μL of cold RLN buffer with a lower NP40 level per well (0.2% instead of 0.5% NP40). The cells were then scraped and transferred to Eppendorf tube to incubate on ice for 5 minutes. Centrifugation for 3 min in 750 g, 4°C, followed by separation of nucleus and cytoplasm. Supernatant fraction (cytoplasm) was transferred to new tubes. Re-centrifugation of nucleus and cytoplasm tubes for better separation. RNA was then extracted using Universal RNA Purification Kit (cat #E3598, EURx)

 doi:10.20944/preprints202508.0564.v1

for RT-PCR experiments. For qPCR experiments we used miRNeasy mini kit (cat#217004, Qiagen, Hilden, Germany), following the manufacturer's instructions. All experiments were performed with at least three biological replicates.

Quantitative PCR

TaqMan microRNA Assay

For RT of miR-99b, the TaqMan MicroRNA Revers Transcription Kit (AB-43666596, ThermoFisher) was used according to the manufacturer's instructions. For PCR we used hsa-miR-99b Primers (TaqMan«MicroRNA Assays INV, SM/PC hsa-miR-99b:000436, AB-4427975), and MultiScribeTM Reverse Transcriptase (ThermoFisher).

RT of mRNA

RT of nuclear RNA was performed using the High-capacity cDNA Reverse Transcription Kit (ThermoFisher) according to the manufacturer's instructions, using RT Random Primers, and MultiScribeTM Reverse Transcriptase.

Quantitative PCR Reaction

mRNA and miR-99b levels were measured using the TaqMan Fast Advanced Mix (ThermoFisher) and the following TaqMan Assays with FAM/MGB-NFQ primers/probe: TaqMan MicroRNA Assays INV, SM/PC, hsa-miR-99b_000436 (AB-4427975, ThermoFisher); TaqMan Gene Expression Assays MTO, XS/PC: beta actin: Hs99999903_m1 (AB-4453320); Custom TaqMan Gene Ex Assays, SM/EA, SPACA6-AS1 intron-exon (AB-4331348, ThermoFisher). Primer Fw: 5′ -GCCCCCACCAGCTTTAGTATCT -3′, Rev: 5′- GTCTGCGGCTGGCTCTGT -3′, FAM Probe: 5′-GGAGCTCACAGTCTGA -3′. TaqMan Gene Expression for SPACA6: Custom TaqMan Copy Number Assays, SM/PC: ID APXGYD (AB-4400294, ThermoFisher). Assays were performed according the manufacturer's instructions. Amplification was carried out using a QuantStudio 3 Real-Time PCR System for 40 cycles at annealing temperature of 60°C. Analysis was performed using the delta-delta C_T, $2^{-\Delta\Delta C_T}$ method. All experiments were performed in at least three biological repeats.

Results

Isolation and Sequencing of Spliceosomal RNA from Neuronal Cell Lines

Hundreds of miRNA sequences in supraspliceosomes were identified (Mahlab-Aviv, 2018 #2696; Mahlab-Aviv, 2020 #2817} but their function is not yet established. We tested neuronal-originated established cell lines from glioblastoma (U87MG), and neuroblastoma (SH-SY5Y). We also tested HCN, a cortical neuron cell line, as a model for healthy cell function. We prepared nuclear supernatants, enriched with supraspliceosomes, under native salt conditions, and fractionated each on glycerol gradients as previously described [56] (see Materials and Methods). This isolation protocol preserves the higher order of splicing complexes as shown by electron microscopy [56,65]. The supraspliceosomes sediment at 200S with splicing factors [62,64,66], used as previously to locate the position of the supraspliceosome in these gradients [58,59].

Next, we extracted small RNA (<200 nt) from the SF of each of the neuronal cell-lines, and used the RNA in the SF for constructing a barcoded library of small RNA for further sequencing, as previously described [58,59]. We created three different libraries for biological triplicates from each cell-line. Statistical summary of the RNA-seq libraries is shown in Supplementary **Table S1**. Alignment of these SF sequences to the human transcriptome revealed a complex collection of RNA species, including pre-miRNAs, small nucleolar RNAs (SNORDs) [67], intronic sequences and more. In this study, we only consider reads that are aligned to the hairpin precursor miRNA of the primary miRNA as determined by miRbase [15]. These sequences are referred to as SF-miRNAs.

 doi:10.20944/preprints202508.0564.v1

Changes in Expression of SF-miRNA Sequences in Neuronal Cancer Cells

Sequencing and alignment to all transcriptome and miRNA collections revealed a large complexity of the miRNA sequences. The mapped SF-miRNAs of the three cell lines HCN, U87MG and SH-SY5Y resulted from the raw data that reported on 688 different miRNA sequences. Among them, 455 miRNAs displayed minimal expression level (Supplementary **Table S1**). We also removed measurement that were assigned to miR-6087 (see Materials and Methods). The heatmap includes 455 miRNAs with a minimal read size of 17 nt and a minimal expression of ≥30 CPM across the three cell lines, flowing normalization (Supplementary **Figure S1**). The number of counts were normalized among cells (see Materials and Methods). The heatmap scaling from 9 samples is a log10 transformation of the expression counts (Supplementary **Figure S1**). We concluded that the nuclear miRNA sequences in all three cell lines are substantially different with higher diversity of miRNAs in SH-SY5Y relative to U87MG, and the most restricted set of miRNAs are associated with HCN.

Figure 1A presents the reads of the raw data of SF-miRNAs observed among the 3 tested cell-lines. Based on the thresholds used for reliable sequenced reads, we identified 155, 227, and 374 SF-miRNAs in HCN, U87MG, and SH-SY5Y cells, respectively (**Figure 1B**). We find that 74 miRNA sequences are expressed in all cell-lines (**Figure 1C)**. The highest expressing miRNAs include miR-1246, miR-21, miR-20a, miR-7704, let-7c, and additional let-7 family members (Supplementary **Table S2**). When testing the miRNAs that are shared in both HCN and U87MG, an additional 14 miRNAs were found, among them are: miR-222, miR-221, and miR-100. Additional 31 SF-miRNAs are shared between HCN and SH-SY5Y (e.g., miR-24-1, miR-24-2, miR-218-1, miR-218-2 miR-27b and miR-269-2). For the two cancerous cell-lines (U87MG and SH-SY5Y) additional 84 SF-miRNAs were detected (e.g., miR-19b-1, miR-20a, miR-129-2, miR-1291, miR-3198-2, miR-3687).

Figure 1C further shows that many of the miRNAs are exclusively expressed in a specific cell-line. A total of 38, 55, and 185 SF-miRNA are expressed solely in HCN, U87MG, and SH-SY5Y, respectively. Notably, among the SF-miRNA, SH-SY5Y cells are exhibiting twice as many miRNA types relative to HCN cells (**Figure 1B**). A Venn diagram of a subset of SF-miRNA that show 5-fold change (increase or decrease) is presented in **Figure 1D**. We concluded that the type and level of expression of SF-miRNAs signify each neuronal cancer cell lines and determine the specific miRNA-based nature of the cell line.

Comparing the Differential Expression of SF-miRNAs in the Neuronal Cell-Lines

It is known that the average number of miRNA molecules in a cell may vary by 4-5 order of magnitudes [68]. **Figure 2** focusess on the difference in expression of the cellular models used, including the HCN and the cancer-originated cells SH-SY5Y and U87MG. As many as 67 SF-miRNAs had a minimal expression level of ≥50 normalized reads (Supplementary **Table S1**). **Figure 2A** displays the relative expression levels of 27 instances where SF-miRNA differential expression is substantial for SH-SY5Y and U87MG (fold change >|5|). **Figure 2B** compares the expression levels of the top SF-miRNAs in the two neuronal cancerous cell lines, demonstrating that the profile of the SF-miRNAs signifies each of these cancerous cell lines.

 doi:10.20944/preprints202508.0564.v1

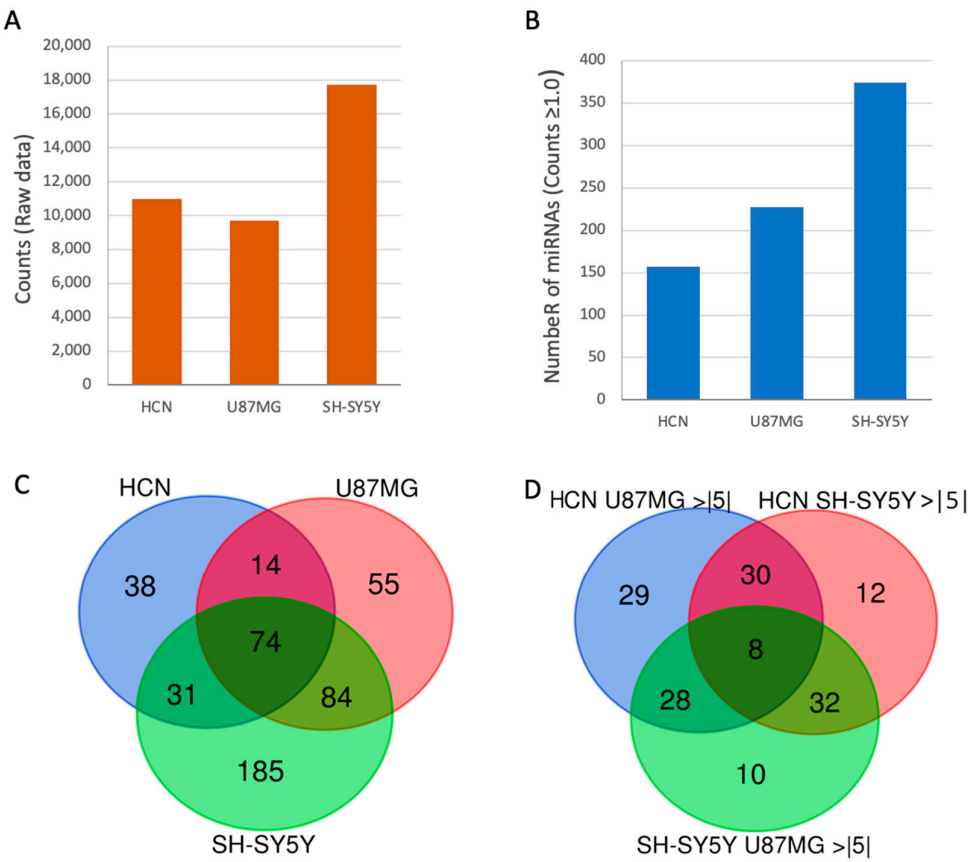

Figure 1. Changes in expression of SF-miRNAs among neuronal cancer - origin cell-lines. **(A**) Changes in number of reads. **(B**) Changes in the number of SF-miRNA of the 3 neuronal cell lines (above a minimal expression level). **(C)** Venn diagram showing the partition of different SF-miRNAs among three neuronal cancer cell-lines. **(D)** Venn diagram showing the partition of different SF-miRNAs among the three neuronal cancer cell-lines showing at least 5xfold change (for up and down regulation).

The analysis further revealed the expression of a large collection of spliceosomal let-7 miRNA in the neuronal cancer cells. The family members of hsa-let-7 (11 miRNAs) were among the most significant SF expressing miRNAs. They account for 28% of all reads from the three cell lines. The difference in the expression is illustrated in **Figure 2C**. For example, in the HCN cell line, the total reads for SF-miRNAs let7 family members were 4.2 times higher than in the other cell lines and account for 57% of all expressed miRNAs in this cell. The dominant type in HCN was hsa-let7c (**Figure 2C**). The differences in composition of SF hsa-let-7 in the different neuronal cell lines is evident, with hsa-let-7g, hsa-let7b and hsa-let7c dominating SH-SY5Y, U87MG and HCN, respectively (**Figure 2D**).

 doi:10.20944/preprints202508.0564.v1

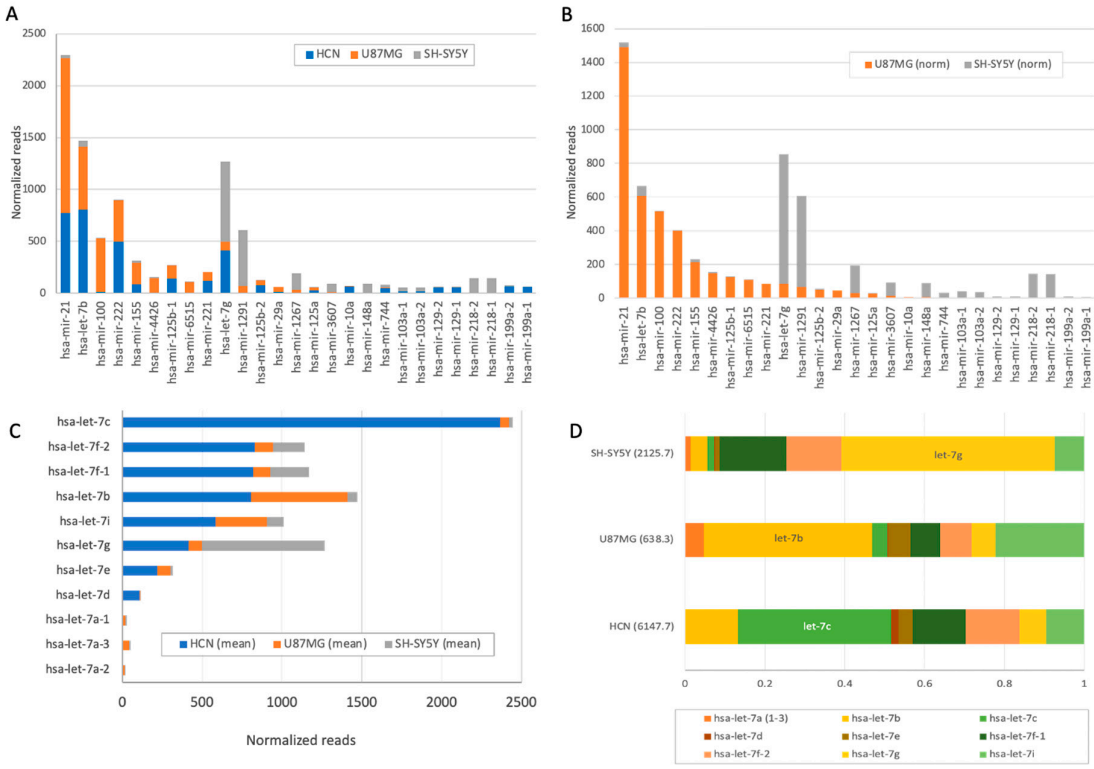

Figure 2. Partition of top SF-miRs in the three neuronal cancer cell lines. (A) Changes in the expression level of the top 27 SF-miRNAs in the three neuronal cell-lines (log scale). The partitions for each miRNA within the three cell-lines is shown. HCN (blue), U87MG (orange) and SH-SY5Y (grey). (B) Changes in the expression level of the top 27 SF-miRNAs in the two neuronal cancer cell-lines (log scale). Note that the highly expressed miR-1246 was excluded for clarity of the visualization. The partitions for each miRNA within the two cell-lines is shown. U87MG (orange) and SH-SY5Y (grey). (C) The partitions of SF-miRNAs for let-7 family members within the three cell-lines is shown. HCN (blue), U87MG (orange) and SH-SY5Y (grey). (D) The relative composition of the different Let-7 SF-miRNA within each of the three neuronal cell-lines is presented. Supplemental Table S2 shows the expression level by cell line for the major let-7 family members.

Table 1 presents the top listed SF-miRNAs ranked by their normalized expression levels in the three neuronal cells (≥150 reads each miRNA) along with their function in cancer of the Central Nervous System (CNS). Among these top listed SF-miRNAs over half showed an increased expression in the cancerous versus normal HCN cell lines (e.g., SF-miR-1246, miR-20a, miR-7704). The opposite direction assigned with a third of the SF-miRNAs (e.g., SF-miR-222, miR-320a, miR-221) and only three instances showed an increased expression in U87MG cells and decreased expression in SH-SY5Y cells compared to the normal HCN cells (SF-miR-21, miR-100 and miR-155).

We concluded that numerous of miRNAs that were implicated with tumor suppressive effects are highly expressed in SF-miRNAs of HCN cells. Furthermore, for about a third of the listed SF-miRNAs, no evidence in CNS tumors were reported.

Table 1. Nuclear SF-miRNAs with total normalized reads ≥150.

SF-miRNA	HCN (%)	U87MG (%)	SH-SY5Y (%)	Total counts	Function in CNS cancer[a]
hsa-mir-1246	3.27	24.73	**72.00**	5963.50	OncomiR: Exosome, Regulates Wnt/β-catenin and TP53
hsa-mir-21	33.77	**64.92**	1.32	2294.20	oncomiR: cell proliferation, invasion

 doi:10.20944/preprints202508.0564.v1

hsa-mir-222	**55.32**	44.66	0.02	898.40	cell cycle progression
hsa-mir-20a	0.77	**59.41**	39.81	816.70	miR-17-92 cluster: oncogenic: proliferation, invasion,
hsa-mir-7704	5.84	**72.12**	22.04	792.60	?, regulating HAGLR
hsa-mir-19b-1	0.25	**60.57**	39.18	788.50	miR-17-92 cluster: oncogenic: proliferation, invasion,
hsa-mir-1291	0.28	11.01	**88.72**	610.60	?
hsa-mir-3198-2	0.00	**54.17**	45.83	593.90	?
hsa-mir-100	2.59	**97.34**	0.09	529.90	tumor suppressor, targeting mTOR, FGFR3, and IGF1R.
hsa-mir-3687	0.87	41.31	**57.84**	423.60	?
hsa-mir-92a-1	13.35	**51.31**	35.36	417.10	miR-17-92 cluster: oncogenic: proliferation, invasion,
hsa-mir-92a-2	14.68	**50.37**	34.92	374.60	miR-17-92 cluster: oncogenic: proliferation, invasion,
hsa-mir-320a	47.03	30.14	22.83	360.00	tumor suppressor: inhibit angiogenesis and migration.
hsa-mir-155	26.82	**67.58**	5.60	314.30	immune response, STAT3 signalling
hsa-mir-27b	**78.53**	5.81	15.69	302.70	conflict: anti-migration. apoptosis, stemness
hsa-mir-125b-1	**52.31**	45.70	1.99	270.90	inhibiting proliferation and regulate apoptosis
hsa-mir-221	**58.17**	41.83	0.00	206.30	driving proliferation, survival, invasion, apoptosis
hsa-mir-3064	7.24	41.43	**51.33**	203.00	?
hsa-mir-1267	0.00	16.05	**83.95**	195.00	?
hsa-mir-423	29.02	37.62	33.37	193.00	cell growth via p21 and p53-related pathways
hsa-mir-24-2	**81.85**	5.85	12.30	182.90	tumor-suppressive effects
hsa-mir-26a-1	**73.28**	11.12	15.67	158.30	tumor-suppressive effects
hsa-mir-26a-2	**71.48**	12.16	16.36	157.10	tumor-suppressive effects
hsa-mir-4426	0.00	**95.90**	4.10	153.80	?

[a]**Function reported from CNS cancer, when available; ?, unknown function or under-studied.** In bold face, the cell line that dominates the signal of this SF-miRNA with >50% of the reads.

Glioma and Glioblastoma Expression Trends

We have analyzed the expression trend of miRNAs as reported by miRCancer [69]. The two most common CNS cancer are defined as glioblastoma and glioma (lower grade glioma, diffuse glioma). These cancer types differ greatly in their aggressive nature and cell type origin. While glioma may originate from astrocytomas, oligodendrogliomas and ependymomas cells, the glioblastoma (GBM) is a highly invasive astrocytoma of type IV with poor prognosis. We seek coherence between these major human CNS cancers and the differentially expressed miRNAs (DEMs) between the neuronal cancerous cell lines of SH-SY5Y and U87MG (**Figure 3**).

The overlap list is indicated in the Venn diagrams and colored by the annotation provided by each of the cell lines (up or down regulation relative to HCN, colored red and green, respectively). For a large fraction of our findings, the expression trend reported by miRCancer (based on compilation from the literature, Supplementary **Table S3**) contradict with the SF-miRNAs trends in our cell lines. For example, for the SH-SY5Y, there are 9 common SF-miRNAs, among them miR-21,

 doi:10.20944/preprints202508.0564.v1

miR-221, and miR-622 displays opposite direction, with miR-146b and miR-222 that only agree with the trend in one of the two diseases. Furthermore, 6 SF-miRNAs show contradictory trend with Glioma, and a single SF-miRNA (miR-330) with Glioblastoma (**Figure 3,** left). A similar observation applied also for the U87MG analysis (**Figure 3**, right). Among the 6 common SF-miRNAs miR-100, and miR-198 show opposite direction to miRCancer, while miR-146b only agree with the trend in one of the two diseases, and 5 additional SF-miRNAs show opposite trend to Glioma. While the number of SF-miRNAs that met the Glioblastoma trend for both SH-SY5Y and U87MG is smaller than for the Glioma trend (6 and 3, compared to 13, and 11, respectively), the results are quite consistent, excluding miR-330 that is upregulated in SH-SY5Y, but downregulated in miRCancer reported literature. We noted that in some instances, the report in miRCancer is conflicting (a conflict is defined by having >10% of the literature reports in opposite expression trend). However, even when excluding these instances (marked by a question mark, **Figure 3**), in over 50% of the cases, an opposite trend in expression was evident. We concluded that many of these reported SF-miRNAs (that were significantly expressed with respect to HCN cells), carry yet unknown functions which are different from that in the cytoplasm, and likely that these functions are relevant to the sub-localization of the miRNA sequences in the spliceosome fraction.

Based on the miRCancer analysis that is based on ample evidence from of the literature, we concluded that the subcellular location of miRNAs in the nucleus and specifically at the SF, is a strong indicator for their unique role in the nucleus, irrespectively to the classical cytoplasmic impact of miRNAs on the ribosome level and translation.

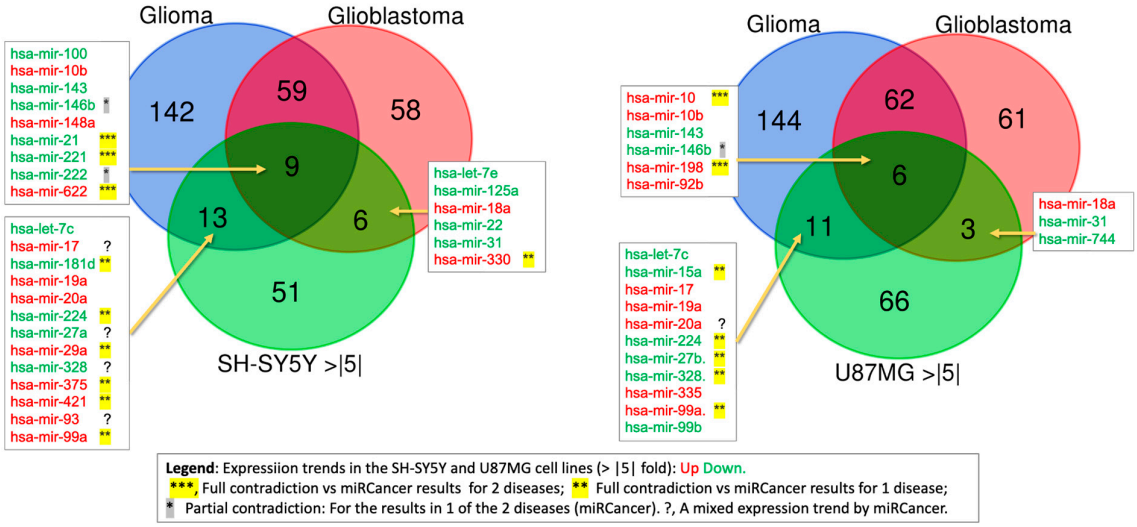

Figure 3. Overlap of miRNA expression trend from CNS cancer and SF-miRNAs from cancerous cell lines. The Venn diagram shows the overlap between differentially expressed SF-miRNAs (≥5-fold change) in SH-SY5Y (left) or U87MG (right) cell lines, and miRNAs reported in miRCancer database for glioma and glioblastoma. Names of the miRNAs are listed, with the colours marking the expression trend. Up and Down regulation are indicated with red and green font, respectively. The analysis SH-SY5Y and U87MG cell lines (>|5| fold). The legend indicates the symbols that describes the degree of contradiction of cell line expression trend and the miRCancer data.

Changes in the Segmental Regions of SF-miRNA in Neuronal Cancer Cell-Lines

We illustrate the analysis of segmental composition in all tested cell lines. **Figure 4A** shows the partition of a prototype precursor miRNA to segments (classified to 5 groups). While 4 segmental groups refer to segments within the pre-miRNA transcript, the extended segment refers to genomic sequences at the margins of the precursor group.

 doi:10.20944/preprints202508.0564.v1

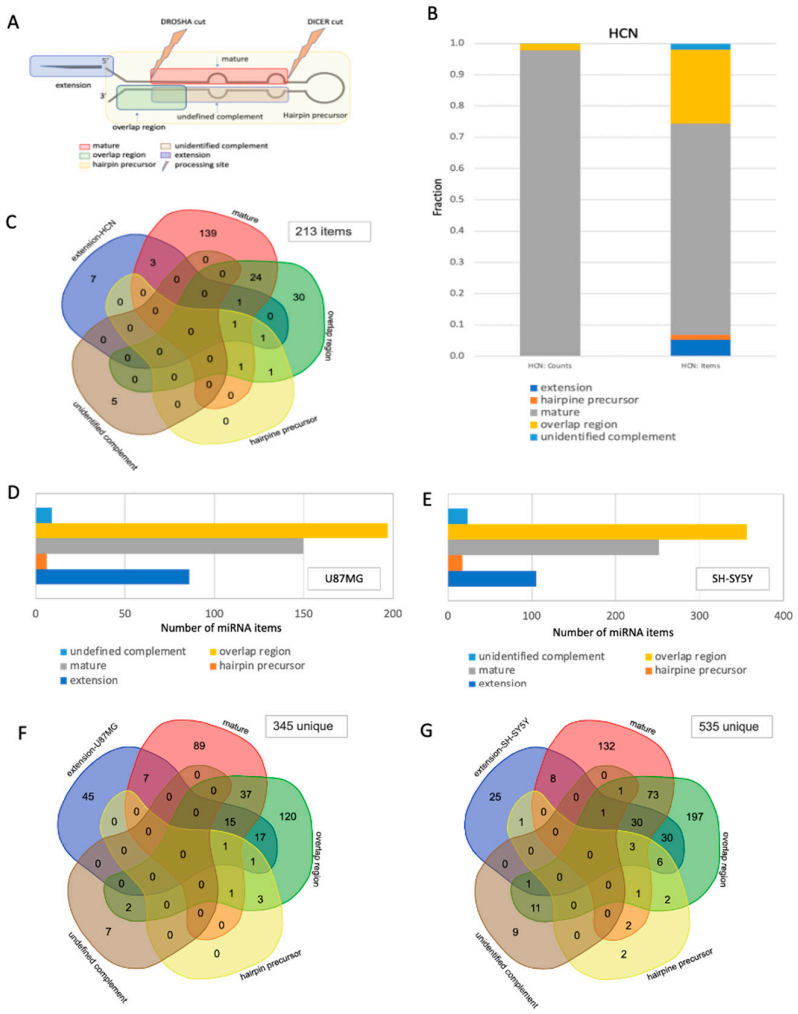

Figure 4. Segmental profile of SF-miRNAs in neuronal cancer cell lines. (A) A schematic view of a miRNA prototype, where the different regions of the pre-miRNA are listed according to their positions relative to the pre-miRNA's major processing sites. An example of an overlap region, defined as reads that cross known segmental border, is indicated. **(B)** The relative counts of reads mapped to each of the predefined regions for the HCN cell line. The relative counts of reads in each of the pre-miRNA regions are color-coded as detailed. Total counts of reads (left) and items (right) are shown. **(C)** Venn diagram showing the overlap between different segmental groups of SF-miRNA within the HCN cell line. There are 213 unique items. Among the possible 32 sections of the Venn, 20 are marked as zero (i.e., no shared segmental groups). The most significant overlap is associated with the mature and overlap region groups. **(D)** Histogram showing the number of items for the U87MG cell line, categorized by the five types of segment groups. The overlap region is the dominant group. **(E)** Histogram showing the number of items for the SH-SY5Y cell line, categorized by the five types of segment groups. The overlap region is the dominant group. **(F)** Venn diagram showing the overlap between different segmental groups of SF-miRNA within the U87MG cell line. There are 345 unique items. Among the possible 32 sections of the Venn, the most significant overlap is associated with the mature, overlap region, and extension groups. **(G)** Venn diagram showing the overlap between different segmental groups of SF-miRNA within the SH-SY5Y cell line. There are 535 unique items. The most significant overlap is associated with the mature, overlap region, and extension groups. Only 11 of the 32 sections have no shared segments (marked as zero). The data source is found in Supplemental **Table S4**.

In the case of the HCN cell line**, Figure 4B** shows that almost all the SF-miRNA-derived sequences are assigned to mature miRNA (98%). By accounting only for the number of unique items

 doi:10.20944/preprints202508.0564.v1

(total 250 items), the fraction of overlap regions, and other segments is more substantial (33%). **Figure 4C** provides a detailed analysis of the overlaps between different segmental groups. We observed that the mature miRNAs and overlap regions show substantial overlap, while the rest of the segmental types are negligible. Altogether there were 250 references of SF-miRNAs that accounts for 213 unique items (due to having the same miRNA with more than one segmental group).

The occurrence of 30 SF-miRNAs that are only identified as overlap regions and the SF-miRNAs that show evidence of unidentified complement sequences (miR-1281, miR-636, miR-4737, miR-555, and miR-3685) highlight alterations in processing and potential role for nonconventional transcripts at the spliceosome.

Unlike SF-miRNA in HCN cells, in which most of the types are of mature miRNA, in both neuronal cancer cells (U87MG and SH-SY5Y) the majority of SF-miRNA are of overlap sequences (**Figures 4D-4E**). A detailed analysis of the overlaps among segmental groups in U87MG (**Figure 4F**) and SH-SY5Y (**Figure 4G)** shows that the trend in both cancerous neuronal cells is quite identical, with the main segmental regions are of overlap regions followed by mature sequences. It should be noted that in HCN (**Figure 4C**), U87MG (**Figure 4F**) and SH-SY5Y (**Figure 4G**) we identified among the SF-miRNA 5, 7 and 9 unidentified complement segments, respectively.

Spliceosomal miR-99b Inhibits Splicing of the lncRNA SPACA6-AS1

An interesting case of potential crosstalk through RNA:RNA base-pairing between an SF-miRNA and a transcript expressed from the same genomic region, yet, in the opposite direction, is the case of miR-99b (**Figure 5A)**. The mir-99b is a member of a cluster of miRNAs (miRNA-99b, let-7e and miRNA-125a), which is antisense to SPACA6-AS1 **(Figure 5A**). miR-99b is positioned in intron 1 of an isoform of the SPACA6 gene (Sperm acrosome associated 6). Notably, miR-99b fully complements the 5′ splice junction of intron 1 of SPACA6-AS1, which is transcribed in the antisense direction of SPACA6 and miR-99b. SPACA6-AS1 (also termed LINC01129, SPACA6p-AS) is a long non-coding RNA (ncRNA) for which very little is known and according to GTEx data, its expression is detected in testis (Supplementary **Figure S2**). It is considered as a risk lncRNA, inversely related to breast cancer survival [70]. SPACA6-AS1 also forms a competing endogenous RNA (ceRNA) network, involving miR-125a and its mRNA targets (Lin28b, MMP11, SIRT7, Zbtb7a) in hepatocarcinoma cells. In the latter cells, miR-125a can regulate the expression of SPACA6-AS1 and vice versa, and overexpression of SPACA6-AS1 regulates onco-suppressive miR-125a, resulting in upregulation of its oncogenic targets [71].

Because miR-99b is fully complementary to the 5′ splice junction of intron 1 of SPACA6-AS1, spanning positions -6 to +16 relative to the junction and likely forming a 22-nt duplex, this complementarity suggests that SF-miR-99b can inhibit the splicing of SPACA6-AS1 by competing with the binding of U1 and U6 snRNPs, both required for splicing of this lncRNA. A crosstalk between SF-miR-99b and SPACA6-AS1 has been proposed [58], in which SF-miR-99b affects both its own expression level and the splicing of SPACA6-AS1 pre-mRNA by acting as a splicing inhibitor. While miR-99b targets the 5′ splice junction of SPACA6-AS1, let-7e and miR-125a are complementary to its exon 1.

 doi:10.20944/preprints202508.0564.v1

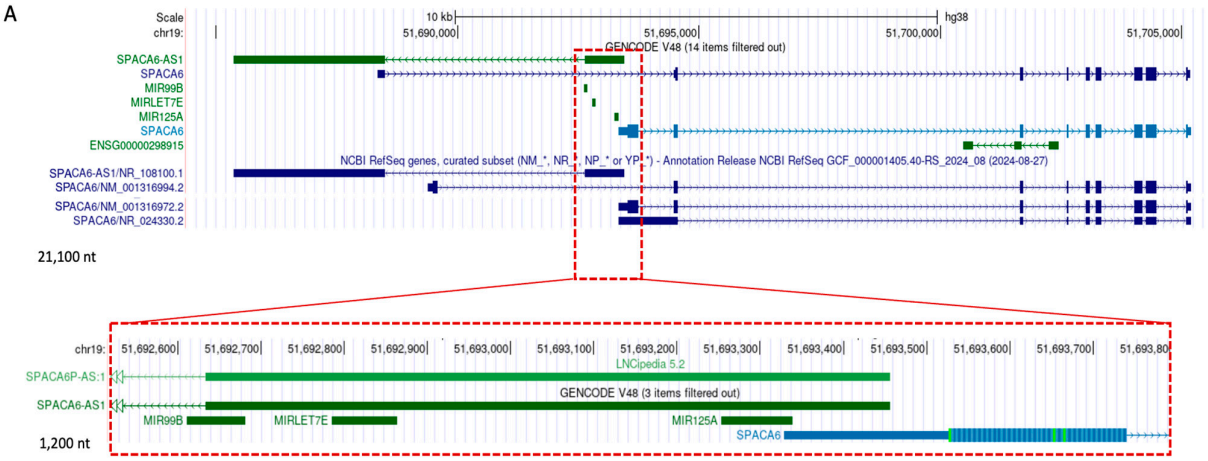

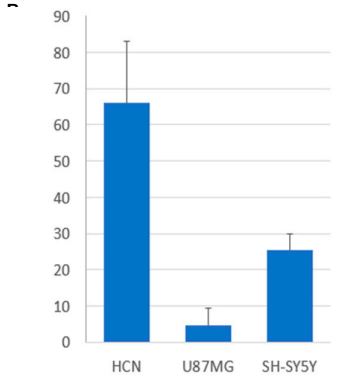

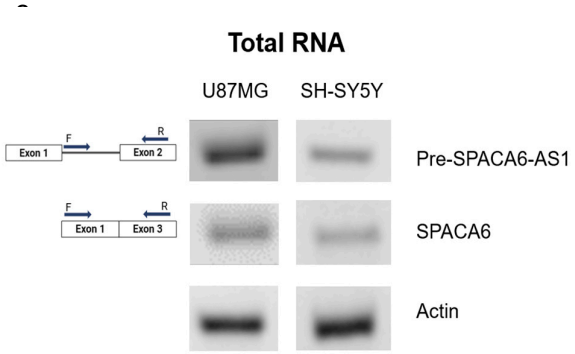

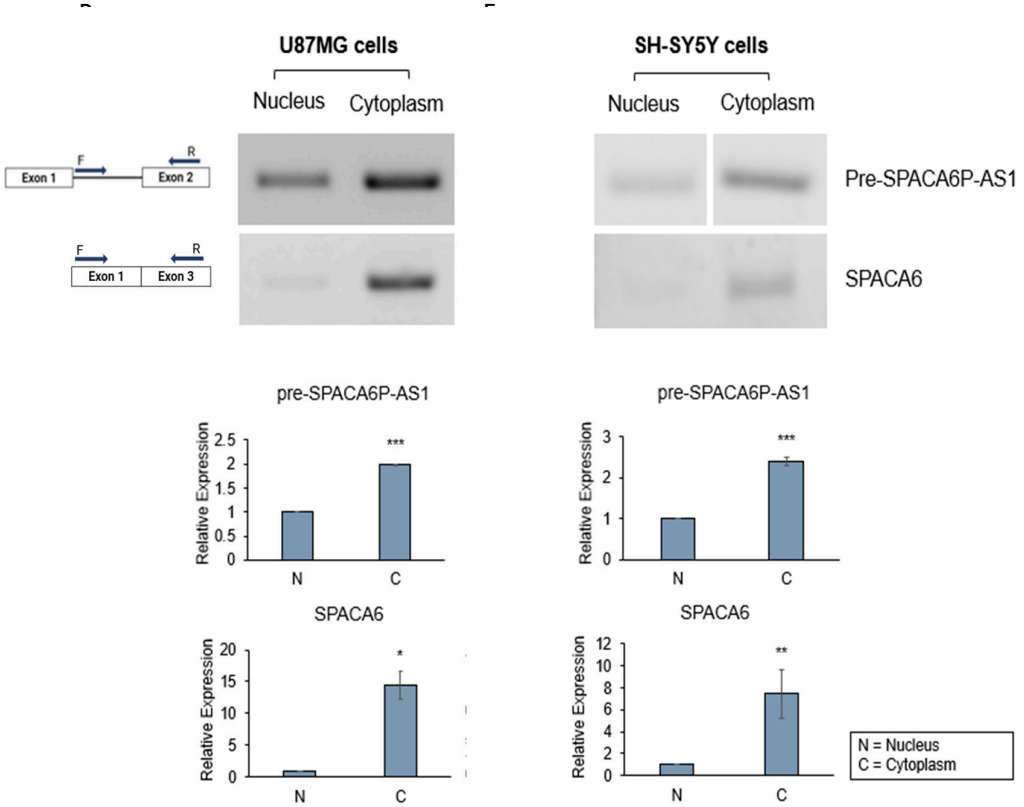

 doi:10.20944/preprints202508.0564.v1

Figure 5. Genomic and gene expression **Figure 5.** Genomic and gene expression views on SPACA6-AS1 pre-mRNA and the genomic miR-99b in neuronal cancer cells. **(A)** Genome browser view of 22,000 nt from Chr19 covering SPACA6 and SPACA6-AS1. The miR-99b cluster is indicated by the dashed red frame, and zoom-in (red dashed frame) of the 1250 nt around the miR-99b cluster. The ability of miR-99b-5p to completely complement by base-pairing to the 5′ splice junction of the intron of SPACA6-AS1, which is transcribed in the antisense direction of SPACA6 is shown. (**B)** RNA-Seq results of SF-miR-99b of the three neuronal cell-lines. **(C)** Results from the RT-PCR analysis of SPACA6 and SPACA6-AS1 pre-mRNA expression from total RNA extracted from the U87MG and SH-SY5Y cell lines are shown. **(D)** RT-PCR analysis of RNA extracted from nuclear and cytoplasmic fractions of the U87MG cell-line for the expression of pre-SPACA6-AS1 and SPACA6 (upper panel). Bars represent quantitation of three biological repeats of the respective RT-PCR analyses (lower panel). **(E)** RT-PCR analysis of RNA extracted from nuclear and cytoplasmic fractions of the SH-SY5Y cell-line for the expression of pre-SPACA6-AS1 and SPACA6 (upper panel). Bars represent quantitation of three biological repeats of the respective RT-PCR analyses (lower panel).

RNA-Seq of SF-miRNA in the three neuronal cell lines (**Figure 5B**) revealed that the expression level of miR-99b is lower in the neuronal cancer cells compared to the normal HCN cells. The expression level of the other two spliceosomal SF-miRNAs, miR-125 and Let-7e, also decrease in the cancer cell lines compared to the normal HCN cells (Supplementary **Table S1**). Because each of the three neuronal cell lines is distinct, we focused on each of them separately, and tested the effect of miR-99b on each of these two cell lines (The HCN cell line is discontinued and thus was not analysed for the effect of miR-99b). RT-PCR analysis of total RNA from the U87MG cells revealed the expression of pre-SPACA6-AS1 and SPACA6. Low levels of pre-SPACA6-AS1 and SPACA6 were found in total RNA from SH-SY5Y cells (**Figure 5C**). We next asked if the pre-SPACA6-AS1 is exported to the cytoplasm in the neuronal cancer cells, or it is retained in the nucleus. For this aim we isolated nuclei and cytoplasm from each of the neuronal cancer cells (see Materials and Methods, Supplementary **Figure S3**) and analysed the expression of pre-SPACA6-AS1 and SPACA6 by RT-PCR. **Figures 5D-5E** show that pre-SPACA6-AS1 is found in both the nucleus and cytoplasm in both neuronal cancer cells, but the majority is exported to the cytoplasm.

To test the effect of miR-99b on the splicing of SPACA6-AS1, we analysed the effect of inhibition and overexpression of miR-99b on the expression of SPACA6-AS1 pre-mRNA by qPCR in the two neuronal cancer cell-lines (**Figure 6**). In U87MG cells, inhibition of miR-99b to ~40% resulted in downregulation of pre-SPACA6-AS1, while the effect on the expression of SPACA6 was low. Over expression of miR-99b increased the expression of pre-SPACA6-AS1 by 50%, while slightly decreased the expression of SPACA6 mRNA (**Figure 6A**). In the SH-SY5Y cell-line, similar down regulation of pre-SPACA6-AS1 RNA by inhibition of mir-99b was observed, and a slight increase in expression of SPACA6. Overexpression of miR-99b in SH-SY5Y cells resulted in increased expression of SPACA6-AS1 pre-mRNA and also an increase in the expression of SPACA6 (**Figure 6B**). Because miR-99b displays a full complementary to the 5′-splice-site of SPACA6-AS1, we can conclude that inhibition of miR-99b decreased the inhibition of splicing of SPACA6-AS1 and thus decreased the level of pre-SPACA6-AS1, while overexpression of miR-99b inhibited the splicing of SPACA6-AS1 pre-mRNA. The relatively low effects of overexpression of miR-99b on the level of SPACA6-AS1 pre-mRNA in SH-SY5Y cells could be explained either by the complex effect of the cluster of miRNAs (miR-99b, let-7e and miR-125a) in these cells, or by a high percentage of all SPACA6-AS1 transcripts being precursor molecules in the SH-SY5Y cells, and thus the effect of overexpression of miR-99b on SPACA6-AS1 pre-mRNA is small. We cannot exclude a combination of both explanations, or additional, yet undetermined, causes. These experiments show that the splicing of SPACA6-AS1 pre-mRNA is inhibited by miR-99b, which complements it's 5′ splicing junction.

 doi:10.20944/preprints202508.0564.v1

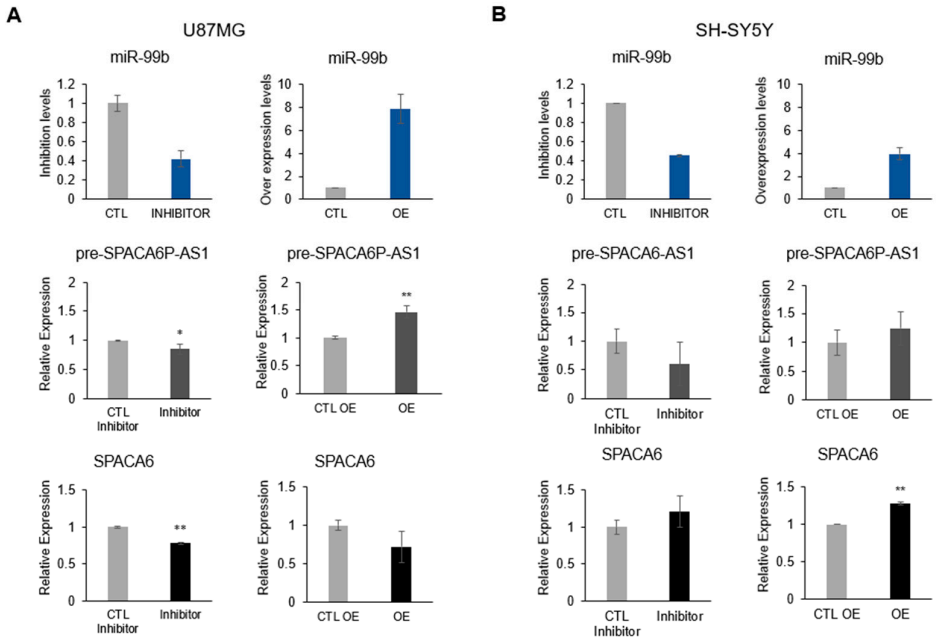

Figure 6. miR-99b increase the level of pre-SPACA6-AS1 in U87mG and SH-SY5Y neuronal cancer cells. The effect of inhibition (left), or overexpression (OE, right) of miR-99b on the nuclear expression of pre-SPACA6-AS1 and SPACA6 mRNA was analysed by real time PCR in U87MG **(A)** and SH-SY5Y **(B)** cell lines. The results of quantitative PCR representative of an independent biological preparations are shown. The expression levels of SPACA6 and SPACA6-AS1 pre-mRNA was normalized to internal control of ß-actin expression from the same sample preparation. CTL, control; OE, overexpression.

Discussion

The crosstalk between miRNA and the spliceosome was already confirmed by the presence of numerous miRNA sequences within the endogenous spliceosome identified by RNA-Seq [49,58,59,72], and also by the finding of the main microprocessor components, Drosha and DGCR8 within [49]. We show that not only sequences derived from intronic miRNA were found in supraspliceosomes, but also rich collection of sequences derived from autonomously expressed miRNAs, among them many that were involved in cancer [58]. This finding supports the view that in addition to the classical translation suppression that characterizes cytosolic miRNAs, novel functions for miRNA sequences within the endogenous spliceosome emerged. We propose a crosstalk through RNA:RNA base-pairing between a spliceosomal miRNA and a transcript expressed from the same genomic region, yet, in an opposite direction. A support for this hypothesis was provided from the case of miR-7704 whose genomic position overlaps HAGLR, a cancer-related lncRNA. An inverse expression of miR-7704 and HAGLR was shown in breast cancer cell lines [59]. Moreover, inhibition of miR-7704 caused an increase in HAGLR expression in both cervical [58] and breast cancer cell lines [59]. Furthermore, overexpression of miR-7704 decreased HAGLR expression in a cervical cancer cell line [58]. Importantly, several SF-miRNAs from breast cancer cells show opposite trend to what is known from miRCancer including the case of SF-miR-7704. Thus, the spliceosomal miR-7704 acts as a tumor-suppressor gene and the oncogenic lncRNA HAGLR being its nuclear target [59].

In this study, by analyzing spliceosomal miRNA in the neuronal cell-lines, we provide further support to the novel role of SF-miRNAs as nuclear target in neuronal context (**Figures 1, 2** and **Table 1**), where we validate changes between cancer-derived cell lines and normal cells.

 doi:10.20944/preprints202508.0564.v1

Spliceosome-associated miRNAs mark neuronal cancer cells. Each of the neuronal cell-lines is signified by the level of expression of miRNA sequences, the number of types miRNA sequences and their pre-miRNA segmental region. There are more types of miRNAs in the neuronal cancer cells compared to the normal HCN cells (155, 227, and 374 SF-miRNAs in HCN, U87MG, and SH-SY5Y, respectively; **Figure 1B**), with the highest expressing SF-miRNAs including miR-1246, miR-21, miR-20a, miR-7704, let-7c, and additional let-7 family members (Supplementary **Table S2**). While 74 miRNAs are common to the three neuronal cell lines, some of the SF-miRNAs are specific to only one of the neuronal cell lines (38, 55, 185 are specific to HCN, U87MG and SH-SY5Y, respectively; **Figure 1**). Notably, the let-7 family are highly represented among the SF-miRNA in the 3 neuronal cell lines, with each neuronal cell line having a specific expression pattern of let-7 family members. Specifically, SF-let-7c, SF-let-7b and SF-let-7g being the top let-7 family member among the SF-miRNAs in HCN, U87MG and SH-SY5Y, respectively (**Figure 2**).

We compared the expression trend of miRNAs as reported by miRCancer [69] for glioblastoma and glioma, major human CNS cancers, and the differentially expressed miRNAs (DEMs) between the neuronal cancerous cell lines of SH-SY5Y and U87MG (**Figure 3**). The analysis revealed that of the 9 SF-miRNA common to SH-SY5Y and glioma and glioblastoma, 3 show opposite trend to miRCancer (SF-miR-21, sF-miR-221, SF-miR-622) while 2 (SF-miR-146b, SF-miR-222) show opposite trend to only one of the cancers. Furthermore, 6 of the 13 SF-miRNAs common to SH-SY5Y and glioma exhibit opposite trend with glioma, and a single SF-miRNA also to glioblastoma. The comparison between SF-miRNA in U87MG cells and miRCancer data show similar trends, yet with smaller number of discrepancies, in view of the smaller number of SF-miRNAs in this cell-line (**Figure 1**). Overall, of the 28 SF-miRNAs shared between SH-SY5Y cells and one or the two diseases, 3 show opposite trend to the two diseases (SF-miR021, SF-mir-221, SF-miR-622), and 9 SF-miRNA show opposite trend to one of the diseases. In the U87MG cell line, of the 20 SF-miRNA shared with one or the two diseases, 2 (SF-miR-100, SF-miR-198) show opposite trend to the two diseases, and 6 show opposite trend to one of the diseases. The abundance of instances with an opposite trend indicates a different nuclear target for the SF-miRNA than the cytoplasmic one. An option for nuclear target of SF-miRNA that comes to mind is through complementarity to a genomic sequence not related to the genomic location of the miRNA. An example is SF-miR-320a which is complementary to the promoter of RNA PolIII D subunit (POLR3D). An inverse correlation between the expression of miR-320a and POLR3D in a number of cell lines was shown. Furthermore, transfection of HEK293 cells with miR-320a led to silencing of POLR3D at the nucleus [36]. In the neuronal cells we find decrease in the expression of miR-320a with cancer (**Table 1**).

Search for nuclear miRNAs complementarity in human promoters revealed numerous additional targets, suggesting that they may function in transcription inhibition [37]. Another option is through complementarity of the SF-miRNA to a nuclear transcript (e.g., pre-mRNA), independent of the genomic location of that transcript (see below). Additional option is through full complementarity of the SF-miRNA to a transcript expressed from the same genomic region, yet in the opposite direction, such as was shown for SF-miR-7704 and the lncRNA HAGLR [58,59].

The top SF-miRNA in the neuronal cancer cells is miR-1246, which was shown to have oncogenic roles in a large number of cancers including glioma (reviewed in ref [73]). It is also upregulated in the neuronal cancer cells with the highest level in the SH-SY5Y neuroblastoma cell line. In addition to the cytoplasmic reported targets [73], SF-miR-1246 have potential nuclear targets complementing intronic sequences in over 20 pre-mRNAs. One potential target is KAZN (Kazrin, periplakin interacting) pre-mRNA. KAZN mRNA encodes for a protein that plays a role in desmosome assembly, cell adhesion, cytoskeletal organization, and epidermal differentiation. It has several alternative isoforms, and thus SF-miR-1246 might play a role in the balance between the different isoforms. Another potential example is JMY (Junction mediating and regulatory protein, p53 cofactor) pre-mRNA. JMY mRNA encodes for a protein that interacts with actin and act as p53 transcription coactivator. SF-miR-1246 which complement intronic sequences in JMY pre-mRNA might affect its splicing. We propose that those SF-miRNA in each of the neuronal cancer cells tested here, which

 doi:10.20944/preprints202508.0564.v1

show opposite trend to what is known from the literature, compiled in miRCancer for glioma and glioblastoma (**Table 1** and **Figure 3**), are potential candidates for novel nuclear targets, which need to be searched for in the future.

In this study we inspect SF-miRNA with full complementarity to a transcript expressed from the same genomic region, yet at an opposite direction. The SF-miR-99b is fully complementary to the 5′ splice junction of lncRNA SPACA6-AS1 pre-mRNA (**Figure 5A**). Very little is known about SPACA6-AS1, which according to GTEx data, its expression is detected in testis (Supplementary **Figure S2**). This lncRNA is a risk lncRNA, inversely related to breast cancer survival [70]. Also, in hepatocarcinoma cells SPACA6-AS1 forms a competing endogenous RNA (ceRNA) network, of miR-125a and its mRNA targets (Lin28b, MMP11, SIRT7, Zbtb7a), where miR-125a can regulate the expression of SPACA6-AS1 and vice versa. Overexpression of SPACA6-AS1 regulates onco-suppressive miR-125a, resulting in upregulation of its oncogenic targets [71].

Using qPCR, we show here that in the neuronal cancer cells U87MG and SH-SY5Y, SF-miR-99b inhibits the splicing of SPACA6-AS1. Inhibition of miR-99b expression resulted in decrease in the level of SPACA6-AS1, while over expression of miR-99b resulted in increase in the level of SPACA6-AS1 pre-mRNA.

Several SF-miRNAs found in ovarian [58], breast cancer [59], and also neuronal cancer cell-lines (this study) overlaps lncRNAs expressed from the same genomic region in an opposite direction. These finding suggest a negative regulation of SF-miRNA of the complementary lncRNA target [61]. One example is the case of miR-7704 which negatively regulates the expression of lncRNA HAGLR in breast cancer cells [59]. Another example is SF-miR-99b, which inhibits the splicing of SPACA6-AS1 pre-mRNA in neuronal cancer cells (**Figures 5, 6**). We can conclude that cases of base pairing of SF-miRNA with complementary RNA sequences, expressed from the same genomic region, yet in an opposite direction, present potential novel nuclear targets against cancer, yet to be explored.

Supplementary Materials: The following supporting information can be downloaded at website of this paper posted on Preprints.org, Supplementary **Table S1** - Statistical summary of the RNA-seq covering 688 miRNAs. Supplementary **Table S2** - Expression of has-let-7 family members. Supplementary **Table S3** - miRCancer results for two CNS diseases. Supplementary **Table S4** - Segmental profile of SF-miRNAs in neuronal cancer cell lines. **Figure S1**. Heatmap of the SF-miRNA of the 3 neuronal cell lines. **Figure S2**. Expression profile of body map of GTEx. **Figure S3**. Isolation of nuclear and cytoplasmic fractions from U87MG and SH-SY5Y cell-lines.

Author Contributions: R.S. and M.L. conceived and designed the study. M.L., S.M.A. and K.Z., performed the bioinformatic analyses. S.M.A. performed the initial data analysis, statistical analyses, of the RNA-Seq data and visualization; S.M.A. and M.L. performed the visualization, annotation and data curation. M.A. supervised the experiments; K.O.S and A.R.P. performed the experiments; R.S., and M.L. designed the RNA-Seq experiments. R.S. and M.L. wrote the paper. All authors discussed the findings, and contributed to the final manuscript.

Funding: This research was partially funded by the Israel Cancer Research Fund (ICRF) Acceleration Grant (R.S), STEP (Science Training Encouraging Piece) fellowship (K.O.S), The Ministry of Science and Technology, Israel, Yitzhak Navon fellowship (M.A), Center for Data Science (CIDR) at the Hebrew University (M.L.) and the Clore Foundation fellowship (K.Z).

Institutional Review Board Statement: The analysed RNA-seq data were added to ArrayExpress and the data accession number is E-MTAB-15383.

Acknowledgments: We would like to thank Aviva Petcho for excellent technical assistance. We thank the system team of the Computer Science and Engineering at the Hebrew University for their support, and The Center for Genomic Technologies, at the Institute of life Sciences at the Hebrew University.

Conflicts of Interest: The authors declare no conflict of interest.

References

1. Di Leva, G., Garofalo, M. and Croce, C.M. (2014) microRNA in cancer. Annu Rev Pathol, 9, 287-314.

 doi:10.20944/preprints202508.0564.v1

2. Loh, H.Y., Norman, B.P., Lai, K.S., Rahman, N., Alitheen, N.B.M. and Osman, M.A. (2019) The Regulatory Role of MicroRNAs in Breast Cancer. *International journal of molecular sciences*, **20**, 4940.
3. Bartel, D.P. (2009) MicroRNAs: target recognition and regulatory functions. *Cell*, **136**, 215-233.
4. Fabian, M.R. and Sonenberg, N. (2012) The mechanics of miRNA-mediated gene silencing: a look under the hood of miRISC. *Nature structural & molecular biology*, **19**, 586-593.
5. Krol, J., Loedige, I. and Filipowicz, W. (2010) The widespread regulation of microRNA biogenesis, function and decay. *Nat Rev Genet*, **11**, 597-610.
6. Ha, M. and Kim, V.N. (2014) Regulation of microRNA biogenesis. *Nat Rev Mol Cell Biol*, **15**, 509-524.
7. Bartel, D.P. (2018) Metazoan MicroRNAs. *Cell*, **173**, 20-51.
8. Gregory, R.I., Yan, K.P., Amuthan, G., Chendrimada, T., Doratotaj, B., Cooch, N. and Shiekhattar, R. (2004) The Microprocessor complex mediates the genesis of microRNAs. *Nature*, **432**, 235-240.
9. Han, J., Lee, Y., Yeom, K.H., Kim, Y.K., Jin, H. and Kim, V.N. (2004) The Drosha-DGCR8 complex in primary microRNA processing. *Genes & development*, **18**, 3016-3027.
10. Han, J., Lee, Y., Yeom, K.H., Nam, J.W., Heo, I., Rhee, J.K., Sohn, S.Y., Cho, Y., Zhang, B.T. and Kim, V.N. (2006) Molecular basis for the recognition of primary microRNAs by the Drosha-DGCR8 complex. *Cell*, **125**, 887-901.
11. Landthaler, M., Yalcin, A. and Tuschl, T. (2004) The human DiGeorge syndrome critical region gene 8 and Its D. melanogaster homolog are required for miRNA biogenesis. *Curr Biol*, **14**, 2162-2167.
12. Lee, Y., Ahn, C., Han, J., Choi, H., Kim, J., Yim, J., Lee, J., Provost, P., Radmark, O., Kim, S. et al. (2003) The nuclear RNase III Drosha initiates microRNA processing. *Nature*, **425**, 415-419.
13. Kim, Y.K. and Kim, V.N. (2007) Processing of intronic microRNAs. *The EMBO journal*, **26**, 775-783.
14. Romano, G., Veneziano, D., Acunzo, M. and Croce, C.M. (2017) Small non-coding RNA and cancer. *Carcinogenesis*, **38**, 485-491.
15. Kozomara, A., Birgaoanu, M. and Griffiths-Jones, S. (2019) miRBase: from microRNA sequences to function. *Nucleic Acids Res*, **47**, D155-D162.
16. He, B., Zhao, Z., Cai, Q., Zhang, Y., Zhang, P., Shi, S., Xie, H., Peng, X., Yin, W., Tao, Y. et al. (2020) miRNA-based biomarkers, therapies, and resistance in Cancer. *Int J Biol Sci*, **16**, 2628-2647.
17. Gabriely, G., Wurdinger, T., Kesari, S., Esau, C.C., Burchard, J., Linsley, P.S. and Krichevsky, A.M. (2008) MicroRNA 21 promotes glioma invasion by targeting matrix metalloproteinase regulators. *Molecular and cellular biology*, **28**, 5369-5380.
18. Gabriely, G., Yi, M., Narayan, R.S., Niers, J.M., Wurdinger, T., Imitola, J., Ligon, K.L., Kesari, S., Esau, C., Stephens, R.M. et al. (2011) Human glioma growth is controlled by microRNA-10b. *Cancer Res*, **71**, 3563-3572.
19. Li, Y., Guessous, F., Zhang, Y., Dipierro, C., Kefas, B., Johnson, E., Marcinkiewicz, L., Jiang, J., Yang, Y., Schmittgen, T.D. et al. (2009) MicroRNA-34a inhibits glioblastoma growth by targeting multiple oncogenes. *Cancer Res*, **69**, 7569-7576.
20. van Wijk, N., Zohar, K. and Linial, M. (2022) Challenging Cellular Homeostasis: Spatial and Temporal Regulation of miRNAs. *International journal of molecular sciences*, **23**, 16152.
21. Ciafre, S.A. and Galardi, S. (2013) microRNAs and RNA-binding proteins: a complex network of interactions and reciprocal regulations in cancer. *RNA biology*, **10**, 935-942.
22. Roberts, T.C. (2014) The MicroRNA Biology of the Mammalian Nucleus. *Molecular therapy*, **3**, e188.
23. Guil, S. and Esteller, M. (2015) RNA-RNA interactions in gene regulation: the coding and noncoding players. *Trends Biochem Sci*, **40**, 248-256.
24. Huang, V. and Li, L.C. (2012) miRNA goes nuclear. *RNA biology*, **9**, 269-273.
25. Liu, H., Lei, C., He, Q., Pan, Z., Xiao, D. and Tao, Y. (2018) Nuclear functions of mammalian MicroRNAs in gene regulation, immunity and cancer. *Mol Cancer*, **17**, 64.
26. Catalanotto, C., Cogoni, C. and Zardo, G. (2016) MicroRNA in Control of Gene Expression: An Overview of Nuclear Functions. *International journal of molecular sciences*, **17**.
27. Liao, J.Y., Ma, L.M., Guo, Y.H., Zhang, Y.C., Zhou, H., Shao, P., Chen, Y.Q. and Qu, L.H. (2010) Deep sequencing of human nuclear and cytoplasmic small RNAs reveals an unexpectedly complex subcellular distribution of miRNAs and tRNA 3' trailers. *PLoS One*, **5**, e10563.

 doi:10.20944/preprints202508.0564.v1

28. Jeffries, C.D., Fried, H.M. and Perkins, D.O. (2011) Nuclear and cytoplasmic localization of neural stem cell microRNAs. *RNA (New York, N.Y*, **17**, 675-686.
29. Ohrt, T., Mutze, J., Staroske, W., Weinmann, L., Hock, J., Crell, K., Meister, G. and Schwille, P. (2008) Fluorescence correlation spectroscopy and fluorescence cross-correlation spectroscopy reveal the cytoplasmic origination of loaded nuclear RISC in vivo in human cells. *Nucleic Acids Res*, **36**, 6439-6449.
30. Ameyar-Zazoua, M., Rachez, C., Souidi, M., Robin, P., Fritsch, L., Young, R., Morozova, N., Fenouil, R., Descostes, N., Andrau, J.C. et al. (2012) Argonaute proteins couple chromatin silencing to alternative splicing. *Nature structural & molecular biology*, **19**, 998-1004.
31. Fasanaro, P., Greco, S., Lorenzi, M., Pescatori, M., Brioschi, M., Kulshreshtha, R., Banfi, C., Stubbs, A., Calin, G.A., Ivan, M. et al. (2009) An integrated approach for experimental target identification of hypoxia-induced miR-210. *The Journal of biological chemistry*, **284**, 35134-35143.
32. Leucci, E., Patella, F., Waage, J., Holmstrom, K., Lindow, M., Porse, B., Kauppinen, S. and Lund, A.H. (2013) microRNA-9 targets the long non-coding RNA MALAT1 for degradation in the nucleus. *Sci Rep*, **3**, 2535.
33. Hansen, T.B., Wiklund, E.D., Bramsen, J.B., Villadsen, S.B., Statham, A.L., Clark, S.J. and Kjems, J. (2011) miRNA-dependent gene silencing involving Ago2-mediated cleavage of a circular antisense RNA. *The EMBO journal*, **30**, 4414-4422.
34. Tang, R., Li, L., Zhu, D., Hou, D., Cao, T., Gu, H., Zhang, J., Chen, J., Zhang, C.Y. and Zen, K. (2012) Mouse miRNA-709 directly regulates miRNA-15a/16-1 biogenesis at the posttranscriptional level in the nucleus: evidence for a microRNA hierarchy system. *Cell Res*, **22**, 504-515.
35. Nishi, K., Nishi, A., Nagasawa, T. and Ui-Tei, K. (2013) Human TNRC6A is an Argonaute-navigator protein for microRNA-mediated gene silencing in the nucleus. *RNA (New York, N.Y*, **19**, 17-35.
36. Kim, D.H., Saetrom, P., Snove, O., Jr. and Rossi, J.J. (2008) MicroRNA-directed transcriptional gene silencing in mammalian cells. *Proc Natl Acad Sci U S A*, **105**, 16230-16235.
37. Younger, S.T., Pertsemlidis, A. and Corey, D.R. (2009) Predicting potential miRNA target sites within gene promoters. *Bioorg Med Chem Lett*, **19**, 3791-3794.
38. Morris, K.V., Santoso, S., Turner, A.M., Pastori, C. and Hawkins, P.G. (2008) Bidirectional transcription directs both transcriptional gene activation and suppression in human cells. *PLoS Genet*, **4**, e1000258.
39. Han, J., Kim, D. and Morris, K.V. (2007) Promoter-associated RNA is required for RNA-directed transcriptional gene silencing in human cells. *Proc Natl Acad Sci U S A*, **104**, 12422-12427.
40. Schwartz, J.C., Younger, S.T., Nguyen, N.B., Hardy, D.B., Monia, B.P., Corey, D.R. and Janowski, B.A. (2008) Antisense transcripts are targets for activating small RNAs. *Nature structural & molecular biology*, **15**, 842-848.
41. Yue, X., Schwartz, J.C., Chu, Y., Younger, S.T., Gagnon, K.T., Elbashir, S., Janowski, B.A. and Corey, D.R. (2010) Transcriptional regulation by small RNAs at sequences downstream from 3′ gene termini. *Nat Chem Biol*, **6**, 621-629.
42. Chi, S.W., Zang, J.B., Mele, A. and Darnell, R.B. (2009) Argonaute HITS-CLIP decodes microRNA-mRNA interaction maps. *Nature*, **460**, 479-486.
43. Shomron, N. and Levy, C. (2009) MicroRNA-biogenesis and Pre-mRNA splicing crosstalk. *J Biomed Biotechnol*, **2009**, 594678.
44. Mattioli, C., Pianigiani, G. and Pagani, F. (2014) Cross talk between spliceosome and microprocessor defines the fate of pre-mRNA. *Wiley interdisciplinary reviews. RNA*, **5**, 647-658.
45. Kataoka, N., Fujita, M. and Ohno, M. (2009) Functional association of the Microprocessor complex with the spliceosome. *Molecular and cellular biology*, **29**, 3243-3254.
46. Shiohama, A., Sasaki, T., Noda, S., Minoshima, S. and Shimizu, N. (2007) Nucleolar localization of DGCR8 and identification of eleven DGCR8-associated proteins. *Experimental cell research*, **313**, 4196-4207.
47. Janas, M.M., Khaled, M., Schubert, S., Bernstein, J.G., Golan, D., Veguilla, R.A., Fisher, D.E., Shomron, N., Levy, C. and Novina, C.D. (2011) Feed-forward microprocessing and splicing activities at a microRNA-containing intron. *PLoS Genet*, **7**, e1002330.
48. Allo, M., Buggiano, V., Fededa, J.P., Petrillo, E., Schor, I., de la Mata, M., Agirre, E., Plass, M., Eyras, E., Elela, S.A. et al. (2009) Control of alternative splicing through siRNA-mediated transcriptional gene silencing. *Nature structural & molecular biology*, **16**, 717-724.

 doi:10.20944/preprints202508.0564.v1

49. Agranat-Tamir, L., Shomron, N., Sperling, J. and Sperling, R. (2014) Interplay between pre-mRNA splicing and microRNA biogenesis within the supraspliceosome. *Nucl Acids Res*, **42**, 4640-4651.
50. Bonnal, S.C., Lopez-Oreja, I. and Valcarcel, J. (2020) Roles and mechanisms of alternative splicing in cancer - implications for care. *Nat Rev Clin Oncol*, **17**, 457-474.
51. Ule, J. and Blencowe, B.J. (2019) Alternative Splicing Regulatory Networks: Functions, Mechanisms, and Evolution. *Molecular cell*, **76**, 329-345.
52. Marasco, L.E. and Kornblihtt, A.R. (2023) The physiology of alternative splicing. *Nat Rev Mol Cell Biol*, **24**, 242-254.
53. Wilkinson, M.E., Charenton, C. and Nagai, K. (2020) RNA Splicing by the Spliceosome. *Annu Rev Biochem*, **89**, 359-388.
54. Sperling, J., Azubel, M. and Sperling, R. (2008) Structure and Function of the Pre-mRNA Splicing Machine. *Structure*, **16**, 1605-1615.
55. Sperling, R. (2017) The nuts and bolts of the endogenous spliceosome. *Wiley interdisciplinary reviews RNA*, **8**, e1377. doi: 1310.1002/wrna.1377.
56. Azubel, M., Habib, N., Sperling, J. and Sperling, R. (2006) Native spliceosomes assemble with pre-mRNA to form supraspliceosomes. *J. Mol. Biol.*, **356**, 955-966.
57. Cohen-Krausz, S., Sperling, R. and Sperling, J. (2007) Exploring the architecture of the intact supraspliceosome using electron microscopy. *J. Mol. Biol.*, **368**, 319-327.
58. Mahlab-Aviv, S., Boulos, A., Peretz, A.R., Eliyahu, T., Carmel, L., Sperling, R. and Linial, M. (2018) Small RNA sequences derived from pre-microRNAs in the supraspliceosome. *Nucleic Acids Res*, **46**, 11014-11029.
59. Mahlab-Aviv, S., K., Z., Y., C., Peretz, A.R., Eliyahu, T., Linial, M. and Sperling, R. (2020), IJMS, Vol. 21, pp. 8132.
60. Sperling, R. (2019) Small non-coding RNA within the endogenous spliceosome and alternative splicing regulation. *Biochim Biophys Acta Gene Regul Mech*, **1862** 194406.
61. Arafat, M. and Sperling, R. (2023) Crosstalk between Long Non-Coding RNA and Spliceosomal microRNA as a Novel Biomarker for Cancer. *Noncoding RNA*, **9**.
62. Raitskin, O., Angenitzki, M., Sperling, J. and Sperling, R. (2002) Large nuclear RNP particles-the nuclear pre-mRNA processing machine. *J. Struct. Biol.*, **140**, 123-130.
63. Bustin, M., Simpson, R.T., Sperling, R. and Goldblatt, D. (1977) Molecular homogeneity of the histone content of HeLa chromatin subunits. *Biochemistry*, **16**, 5281-5285.
64. 64. 1. Di Leva, G.; Garofalo, M.; Croce, C.M. microRNA in cancer. *Annu Rev Pathol* **2014**, *9*, 287-314.
65. Loh, H.Y.; Norman, B.P.; Lai, K.S.; Rahman, N.; Alitheen, N.B.M.; Osman, M.A. The Regulatory Role of MicroRNAs in Breast Cancer. *International journal of molecular sciences* **2019**, *20*, 4940, doi:10.3390/ijms20194940.
66. Bartel, D.P. MicroRNAs: target recognition and regulatory functions. *Cell* **2009**, *136*, 215-233.
67. Fabian, M.R.; Sonenberg, N. The mechanics of miRNA-mediated gene silencing: a look under the hood of miRISC. *Nature structural & molecular biology* **2012**, *19*, 586-593, doi:10.1038/nsmb.2296.
68. Krol, J.; Loedige, I.; Filipowicz, W. The widespread regulation of microRNA biogenesis, function and decay. *Nat Rev Genet* **2010**, *11*, 597-610, doi:10.1038/nrg2843.
69. Ha, M.; Kim, V.N. Regulation of microRNA biogenesis. *Nat Rev Mol Cell Biol* **2014**, *15*, 509-524, doi:10.1038/nrm3838.
70. Bartel, D.P. Metazoan MicroRNAs. *Cell* **2018**, *173*, 20-51, doi:10.1016/j.cell.2018.03.006.
71. Gregory, R.I.; Yan, K.P.; Amuthan, G.; Chendrimada, T.; Doratotaj, B.; Cooch, N.; Shiekhattar, R. The Microprocessor complex mediates the genesis of microRNAs. *Nature* **2004**, *432*, 235-240.
72. Han, J.; Lee, Y.; Yeom, K.H.; Kim, Y.K.; Jin, H.; Kim, V.N. The Drosha-DGCR8 complex in primary microRNA processing. *Genes & development* **2004**, *18*, 3016-3027.
73. Han, J.; Lee, Y.; Yeom, K.H.; Nam, J.W.; Heo, I.; Rhee, J.K.; Sohn, S.Y.; Cho, Y.; Zhang, B.T.; Kim, V.N. Molecular basis for the recognition of primary microRNAs by the Drosha-DGCR8 complex. *Cell* **2006**, *125*, 887-901.
74. Landthaler, M.; Yalcin, A.; Tuschl, T. The human DiGeorge syndrome critical region gene 8 and Its D. melanogaster homolog are required for miRNA biogenesis. *Curr Biol* **2004**, *14*, 2162-2167.

 doi:10.20944/preprints202508.0564.v1

75. Lee, Y.; Ahn, C.; Han, J.; Choi, H.; Kim, J.; Yim, J.; Lee, J.; Provost, P.; Radmark, O.; Kim, S.; et al. The nuclear RNase III Drosha initiates microRNA processing. *Nature* **2003**, *425*, 415-419.
76. Kim, Y.K.; Kim, V.N. Processing of intronic microRNAs. *The EMBO journal* **2007**, *26*, 775-783.
77. Romano, G.; Veneziano, D.; Acunzo, M.; Croce, C.M. Small non-coding RNA and cancer. *Carcinogenesis* **2017**, *38*, 485-491, doi:10.1093/carcin/bgx026.
78. Kozomara, A.; Birgaoanu, M.; Griffiths-Jones, S. miRBase: from microRNA sequences to function. *Nucleic Acids Res* **2019**, *47*, D155-D162, doi:10.1093/nar/gky1141.
79. He, B.; Zhao, Z.; Cai, Q.; Zhang, Y.; Zhang, P.; Shi, S.; Xie, H.; Peng, X.; Yin, W.; Tao, Y.; et al. miRNA-based biomarkers, therapies, and resistance in Cancer. *Int J Biol Sci* **2020**, *16*, 2628-2647, doi:10.7150/ijbs.47203.
80. Gabriely, G.; Wurdinger, T.; Kesari, S.; Esau, C.C.; Burchard, J.; Linsley, P.S.; Krichevsky, A.M. MicroRNA 21 promotes glioma invasion by targeting matrix metalloproteinase regulators. *Molecular and cellular biology* **2008**, *28*, 5369-5380, doi:10.1128/MCB.00479-08.
81. Gabriely, G.; Yi, M.; Narayan, R.S.; Niers, J.M.; Wurdinger, T.; Imitola, J.; Ligon, K.L.; Kesari, S.; Esau, C.; Stephens, R.M.; et al. Human glioma growth is controlled by microRNA-10b. *Cancer Res* **2011**, *71*, 3563-3572, doi:10.1158/0008-5472.CAN-10-3568.
82. Li, Y.; Guessous, F.; Zhang, Y.; Dipierro, C.; Kefas, B.; Johnson, E.; Marcinkiewicz, L.; Jiang, J.; Yang, Y.; Schmittgen, T.D.; et al. MicroRNA-34a inhibits glioblastoma growth by targeting multiple oncogenes. *Cancer Res* **2009**, *69*, 7569-7576, doi:10.1158/0008-5472.CAN-09-0529.
83. van Wijk, N.; Zohar, K.; Linial, M. Challenging Cellular Homeostasis: Spatial and Temporal Regulation of miRNAs. *International journal of molecular sciences* **2022**, *23*, 16152, doi:10.3390/ijms232416152.
84. Ciafre, S.A.; Galardi, S. microRNAs and RNA-binding proteins: a complex network of interactions and reciprocal regulations in cancer. *RNA biology* **2013**, *10*, 935-942, doi:10.4161/rna.24641.
85. Roberts, T.C. The MicroRNA Biology of the Mammalian Nucleus. *Molecular therapy* **2014**, *3*, e188.
86. Guil, S.; Esteller, M. RNA-RNA interactions in gene regulation: the coding and noncoding players. *Trends Biochem Sci* **2015**, *40*, 248-256, doi:10.1016/j.tibs.2015.03.001.
87. Huang, V.; Li, L.C. miRNA goes nuclear. *RNA biology* **2012**, *9*, 269-273, doi:10.4161/rna.19354.
88. Liu, H.; Lei, C.; He, Q.; Pan, Z.; Xiao, D.; Tao, Y. Nuclear functions of mammalian MicroRNAs in gene regulation, immunity and cancer. *Mol Cancer* **2018**, *17*, 64, doi:10.1186/s12943-018-0765-5.
89. Catalanotto, C.; Cogoni, C.; Zardo, G. MicroRNA in Control of Gene Expression: An Overview of Nuclear Functions. *International journal of molecular sciences* **2016**, *17*, doi:10.3390/ijms17101712.
90. Liao, J.Y.; Ma, L.M.; Guo, Y.H.; Zhang, Y.C.; Zhou, H.; Shao, P.; Chen, Y.Q.; Qu, L.H. Deep sequencing of human nuclear and cytoplasmic small RNAs reveals an unexpectedly complex subcellular distribution of miRNAs and tRNA 3' trailers. *PLoS One* **2010**, *5*, e10563, doi:10.1371/journal.pone.0010563.
91. Jeffries, C.D.; Fried, H.M.; Perkins, D.O. Nuclear and cytoplasmic localization of neural stem cell microRNAs. *RNA (New York, N.Y* **2011**, *17*, 675-686, doi:10.1261/rna.2006511.
92. Ohrt, T.; Mutze, J.; Staroske, W.; Weinmann, L.; Hock, J.; Crell, K.; Meister, G.; Schwille, P. Fluorescence correlation spectroscopy and fluorescence cross-correlation spectroscopy reveal the cytoplasmic origination of loaded nuclear RISC in vivo in human cells. *Nucleic Acids Res* **2008**, *36*, 6439-6449, doi:10.1093/nar/gkn693.
93. Ameyar-Zazoua, M.; Rachez, C.; Souidi, M.; Robin, P.; Fritsch, L.; Young, R.; Morozova, N.; Fenouil, R.; Descostes, N.; Andrau, J.C.; et al. Argonaute proteins couple chromatin silencing to alternative splicing. *Nature structural & molecular biology* **2012**, *19*, 998-1004, doi:10.1038/nsmb.2373.
94. Fasanaro, P.; Greco, S.; Lorenzi, M.; Pescatori, M.; Brioschi, M.; Kulshreshtha, R.; Banfi, C.; Stubbs, A.; Calin, G.A.; Ivan, M.; et al. An integrated approach for experimental target identification of hypoxia-induced miR-210. *The Journal of biological chemistry* **2009**, *284*, 35134-35143, doi:10.1074/jbc.M109.052779.
95. Leucci, E.; Patella, F.; Waage, J.; Holmstrom, K.; Lindow, M.; Porse, B.; Kauppinen, S.; Lund, A.H. microRNA-9 targets the long non-coding RNA MALAT1 for degradation in the nucleus. *Sci Rep* **2013**, *3*, 2535, doi:10.1038/srep02535.
96. Hansen, T.B.; Wiklund, E.D.; Bramsen, J.B.; Villadsen, S.B.; Statham, A.L.; Clark, S.J.; Kjems, J. miRNA-dependent gene silencing involving Ago2-mediated cleavage of a circular antisense RNA. *The EMBO journal* **2011**, *30*, 4414-4422, doi:10.1038/emboj.2011.359.

 doi:10.20944/preprints202508.0564.v1

97. Tang, R.; Li, L.; Zhu, D.; Hou, D.; Cao, T.; Gu, H.; Zhang, J.; Chen, J.; Zhang, C.Y.; Zen, K. Mouse miRNA-709 directly regulates miRNA-15a/16-1 biogenesis at the posttranscriptional level in the nucleus: evidence for a microRNA hierarchy system. *Cell Res* **2012**, *22*, 504-515, doi:10.1038/cr.2011.137.
98. Nishi, K.; Nishi, A.; Nagasawa, T.; Ui-Tei, K. Human TNRC6A is an Argonaute-navigator protein for microRNA-mediated gene silencing in the nucleus. *RNA (New York, N.Y* **2013**, *19*, 17-35, doi:10.1261/rna.034769.112.
99. Kim, D.H.; Saetrom, P.; Snove, O., Jr.; Rossi, J.J. MicroRNA-directed transcriptional gene silencing in mammalian cells. *Proc Natl Acad Sci U S A* **2008**, *105*, 16230-16235, doi:10.1073/pnas.0808830105.
100. Younger, S.T.; Pertsemlidis, A.; Corey, D.R. Predicting potential miRNA target sites within gene promoters. *Bioorg Med Chem Lett* **2009**, *19*, 3791-3794, doi:10.1016/j.bmcl.2009.04.032.
101. Morris, K.V.; Santoso, S.; Turner, A.M.; Pastori, C.; Hawkins, P.G. Bidirectional transcription directs both transcriptional gene activation and suppression in human cells. *PLoS Genet* **2008**, *4*, e1000258, doi:10.1371/journal.pgen.1000258.
102. Han, J.; Kim, D.; Morris, K.V. Promoter-associated RNA is required for RNA-directed transcriptional gene silencing in human cells. *Proc Natl Acad Sci U S A* **2007**, *104*, 12422-12427, doi:10.1073/pnas.0701635104.
103. Schwartz, J.C.; Younger, S.T.; Nguyen, N.B.; Hardy, D.B.; Monia, B.P.; Corey, D.R.; Janowski, B.A. Antisense transcripts are targets for activating small RNAs. *Nature structural & molecular biology* **2008**, *15*, 842-848, doi:10.1038/nsmb.1444.
104. Yue, X.; Schwartz, J.C.; Chu, Y.; Younger, S.T.; Gagnon, K.T.; Elbashir, S.; Janowski, B.A.; Corey, D.R. Transcriptional regulation by small RNAs at sequences downstream from 3' gene termini. *Nat Chem Biol* **2010**, *6*, 621-629, doi:10.1038/nchembio.400.
105. Chi, S.W.; Zang, J.B.; Mele, A.; Darnell, R.B. Argonaute HITS-CLIP decodes microRNA-mRNA interaction maps. *Nature* **2009**, *460*, 479-486, doi:10.1038/nature08170.
106. Shomron, N.; Levy, C. MicroRNA-biogenesis and Pre-mRNA splicing crosstalk. *J Biomed Biotechnol* **2009**, *2009*, 594678.
107. Mattioli, C.; Pianigiani, G.; Pagani, F. Cross talk between spliceosome and microprocessor defines the fate of pre-mRNA. *Wiley interdisciplinary reviews. RNA* **2014**, *5*, 647-658, doi:10.1002/wrna.1236.
108. Kataoka, N.; Fujita, M.; Ohno, M. Functional association of the Microprocessor complex with the spliceosome. *Molecular and cellular biology* **2009**, *29*, 3243-3254.
109. Shiohama, A.; Sasaki, T.; Noda, S.; Minoshima, S.; Shimizu, N. Nucleolar localization of DGCR8 and identification of eleven DGCR8-associated proteins. *Experimental cell research* **2007**, *313*, 4196-4207.
110. Janas, M.M.; Khaled, M.; Schubert, S.; Bernstein, J.G.; Golan, D.; Veguilla, R.A.; Fisher, D.E.; Shomron, N.; Levy, C.; Novina, C.D. Feed-forward microprocessing and splicing activities at a microRNA-containing intron. *PLoS Genet* **2011**, *7*, e1002330.
111. Allo, M.; Buggiano, V.; Fededa, J.P.; Petrillo, E.; Schor, I.; de la Mata, M.; Agirre, E.; Plass, M.; Eyras, E.; Elela, S.A.; et al. Control of alternative splicing through siRNA-mediated transcriptional gene silencing. *Nature structural & molecular biology* **2009**, *16*, 717-724.
112. Agranat-Tamir, L.; Shomron, N.; Sperling, J.; Sperling, R. Interplay between pre-mRNA splicing and microRNA biogenesis within the supraspliceosome. *Nucl Acids Res* **2014**, *42*, 4640-4651.
113. Bonnal, S.C.; Lopez-Oreja, I.; Valcarcel, J. Roles and mechanisms of alternative splicing in cancer - implications for care. *Nat Rev Clin Oncol* **2020**, *17*, 457-474, doi:10.1038/s41571-020-0350-x.
114. Ule, J.; Blencowe, B.J. Alternative Splicing Regulatory Networks: Functions, Mechanisms, and Evolution. *Molecular cell* **2019**, *76*, 329-345, doi:10.1016/j.molcel.2019.09.017.
115. Marasco, L.E.; Kornblihtt, A.R. The physiology of alternative splicing. *Nat Rev Mol Cell Biol* **2023**, *24*, 242-254, doi:10.1038/s41580-022-00545-z.
116. Wilkinson, M.E.; Charenton, C.; Nagai, K. RNA Splicing by the Spliceosome. *Annu Rev Biochem* **2020**, *89*, 359-388, doi:10.1146/annurev-biochem-091719-064225.
117. Sperling, J.; Azubel, M.; Sperling, R. Structure and Function of the Pre-mRNA Splicing Machine. *Structure* **2008**, *16*, 1605-1615, doi:10.1016/j.str.2008.08.011.
118. Sperling, R. The nuts and bolts of the endogenous spliceosome. *Wiley interdisciplinary reviews RNA* **2017**, *8*

 doi:10.20944/preprints202508.0564.v1

119. e1377. doi: 1310.1002/wrna.1377, doi:10.1002/wrna.1377.
120. Azubel, M.; Habib, N.; Sperling, J.; Sperling, R. Native spliceosomes assemble with pre-mRNA to form supraspliceosomes. *J. Mol. Biol.* **2006**, *356*, 955-966.
121. Cohen-Krausz, S.; Sperling, R.; Sperling, J. Exploring the architecture of the intact supraspliceosome using electron microscopy. *J. Mol. Biol.* **2007**, *368*, 319-327.
122. Mahlab-Aviv, S.; Boulos, A.; Peretz, A.R.; Eliyahu, T.; Carmel, L.; Sperling, R.; Linial, M. Small RNA sequences derived from pre-microRNAs in the supraspliceosome. *Nucleic Acids Res* **2018**, *46*, 11014-11029, doi:10.1093/nar/gky791.
123. Mahlab-Aviv, S.; K., Z.; Y., C.; Peretz, A.R.; Eliyahu, T.; Linial, M.; Sperling, R. Spliceosome-Associated microRNAs Signify Breast Cancer Cells and Portray Potential Novel Nuclear Targets. IJMS, 2020; Vol. 21, p 8132.
124. Sperling, R. Small non-coding RNA within the endogenous spliceosome and alternative splicing regulation. *Biochim Biophys Acta Gene Regul Mech* **2019**, *1862* 194406, doi:10.1016/j.bbagrm.2019.07.007.
125. Arafat, M.; Sperling, R. Crosstalk between Long Non-Coding RNA and Spliceosomal microRNA as a Novel Biomarker for Cancer. *Noncoding RNA* **2023**, *9*, doi:10.3390/ncrna9040042.
126. Raitskin, O.; Angenitzki, M.; Sperling, J.; Sperling, R. Large nuclear RNP particles-the nuclear pre-mRNA processing machine. *J. Struct. Biol.* **2002**, *140*, 123-130.
127. Yitzhaki, S.; Miriami, E.; Sperling, J.; Sperling, R. Phosphorylated Ser/Arg-rich proteins: Limiting factors in the assembly of 200S large nuclear ribonucleoprotein particles. *Proc. Natl. Acad. Sci. USA* **1996**, *93*, 8830-8835.
128. Kotzer-Nevo, H.; de Lima Alves, F.; Rappsilber, J.; Sperling, J.; Sperling, R. Supraspliceosomes at Defined Functional States Portray the Pre-Assembled Nature of the pre-mRNA Processing Machine in the Cell Nucleus. *Int. J. Mol. Sci.* **2014**, *15*, 11637-11664.
129. Spann, P.; Feinerman, M.; Sperling, J.; Sperling, R. Isolation and visualization of large compact ribonucleoprotein particles of specific nuclear RNAs. *Proc. Natl. Acad. Sci. USA* **1989**, *86*, 466-470.
130. Heinrich, B.; Zhang, Z.; Raitskin, O.; Hiller, M.; Benderska, N.; Hartmann, A.M.; Bracco, L.; Elliott, D.; Ben-Ari, S.; Soreq, H.; et al. Heterogeneous nuclear ribonucleoprotein G regulates splice site selection by binding to CC(A/C)-rich regions in pre-mRNA. *The Journal of biological chemistry* **2009**, *284*, 14303-14315, doi:10.1074/jbc.M901026200.
131. Falaleeva, M.; Pages, A.; Matsuzek, Z.; Hidmi, S.; Agranat-Tamir, L.; Korotkov, K.; Nevo, Y.; Eyras, E.; Sperling, R.; Stamm, S. dual function of C/d box snoRNAs in rRNA modification and alternative pre-mRNA splicing. *Proc Natl Acad Sci U S A* **2016**, *113*, E1625-1634.
132. Pritchard, C.C.; Cheng, H.H.; Tewari, M. MicroRNA profiling: approaches and considerations. *Nat Rev Genet* **2012**, *13*, 358-369, doi:10.1038/nrg3198.
133. Xie, B.; Ding, Q.; Han, H.; Wu, D. miRCancer: a microRNA-cancer association database constructed by text mining on literature. *Bioinformatics* **2013**, *29*, 638-644, doi:10.1093/bioinformatics/btt014.
134. Xu, M.; Chen, Z.; Lin, B.; Zhang, S.; Qu, J. A seven-lncRNA signature for predicting prognosis in breast carcinoma. *Transl Cancer Res* **2021**, *10*, 4033-4046, doi:10.21037/tcr-21-747.
135. Di Palo, A.; Siniscalchi, C.; Mosca, N.; Russo, A.; Potenza, N. A Novel ceRNA Regulatory Network Involving the Long Non-Coding Antisense RNA SPACA6P-AS, miR-125a and its mRNA Targets in Hepatocarcinoma Cells. *International journal of molecular sciences* **2020**, *21*, doi:10.3390/ijms21145068.
136. Zhang, Z.; Falaleeva, M.; Agranat-Tamur, L.; Pages, A.P.; Eyras, E.; E.; Sperling, J.; Sperling, R.; Stamm, S. The 5′ untranslated region of the serotonin receptor 2C pre-mRNA generates miRNAs and is expressed in non-neuronal cells. *Exp Brain Res* **2013**, *230*, 387-394.
137. Ghafouri-Fard, S.; Khoshbakht, T.; Hussen, B.M.; Taheri, M.; Samadian, M. A Review on the Role of miR-1246 in the Pathoetiology of Different Cancers. *Front Mol Biosci* **2021**, *8*, 771835, doi:10.3389/fmolb.2021.771835.
138. Kotzer-Nevo, H., de Lima Alves, F., Rappsilber, J., Sperling, J. and Sperling, R. (2014) Supraspliceosomes at Defined Functional States Portray the Pre-Assembled Nature of the pre-mRNA Processing Machine in the Cell Nucleus. *Int. J. Mol. Sci.*, **15**, 11637-11664.

 doi:10.20944/preprints202508.0564.v1

139. Spann, P., Feinerman, M., Sperling, J. and Sperling, R. (1989) Isolation and visualization of large compact ribonucleoprotein particles of specific nuclear RNAs. *Proc. Natl. Acad. Sci. USA*, **86**, 466-470.
140. Heinrich, B., Zhang, Z., Raitskin, O., Hiller, M., Benderska, N., Hartmann, A.M., Bracco, L., Elliott, D., Ben-Ari, S., Soreq, H. et al. (2009) Heterogeneous nuclear ribonucleoprotein G regulates splice site selection by binding to CC(A/C)-rich regions in pre-mRNA. *The Journal of biological chemistry*, **284**, 14303-14315.
141. Falaleeva, M., Pages, A., Matsuzek, Z., Hidmi, S., Agranat-Tamir, L., Korotkov, K., Nevo, Y., Eyras, E., Sperling, R. and Stamm, S. (2016) dual function of C/d box snoRNAs in rRNA modification and alternative pre-mRNA splicing. *Proc Natl Acad Sci U S A*, **113**, E1625-1634.
142. Pritchard, C.C., Cheng, H.H. and Tewari, M. (2012) MicroRNA profiling: approaches and considerations. *Nat Rev Genet*, **13**, 358-369.
143. Xie, B., Ding, Q., Han, H. and Wu, D. (2013) miRCancer: a microRNA-cancer association database constructed by text mining on literature. *Bioinformatics*, **29**, 638-644.
144. Xu, M., Chen, Z., Lin, B., Zhang, S. and Qu, J. (2021) A seven-lncRNA signature for predicting prognosis in breast carcinoma. *Transl Cancer Res*, **10**, 4033-4046.
145. Di Palo, A., Siniscalchi, C., Mosca, N., Russo, A. and Potenza, N. (2020) A Novel ceRNA Regulatory Network Involving the Long Non-Coding Antisense RNA SPACA6P-AS, miR-125a and its mRNA Targets in Hepatocarcinoma Cells. *International journal of molecular sciences*, **21**.
146. Zhang, Z., Falaleeva, M., Agranat-Tamur, L., Pages, A.P., Eyras, E., E., Sperling, J., Sperling, R. and Stamm, S. (2013) The 5′ untranslated region of the serotonin receptor 2C pre-mRNA generates miRNAs and is expressed in non-neuronal cells. *Exp Brain Res*, **230**, 387-394.
147. Ghafouri-Fard, S., Khoshbakht, T., Hussen, B.M., Taheri, M. and Samadian, M. (2021) A Review on the Role of miR-1246 in the Pathoetiology of Different Cancers. *Front Mol Biosci*, **8**, 771835.